

# ONE-LOOP MATCHING IN THE SMEFT EXTENDED WITH A STERILE NEUTRINO

Mikael Chala<sup>a</sup> and Arsenii Titov<sup>b</sup>

<sup>a</sup>*CAFPE and Departamento de Física Teórica y del Cosmos, Universidad de Granada,  
E-18071 Granada, Spain*

<sup>b</sup>*Dipartimento di Fisica e Astronomia “G. Galilei”, Università degli Studi di Padova  
INFN, Sezione di Padova, Via Francesco Marzolo 8, I-35131 Padova, Italy*

## Abstract

We study the phenomenology of the simplest renormalisable model that, at low energy, leads to the effective field theory of the Standard Model extended with right-handed neutrinos ( $\nu$ SMEFT). Our aim is twofold. First, to contextualise new collider signatures in models with sterile neutrinos so far studied only using the bottom-up approach. And second and more important, to provide a thorough example of one-loop matching in the diagrammatic approach, of which other matching techniques and automatic tools can benefit for cross-checks. As byproducts of this work, we provide for the first time: *(i)* a complete off-shell basis for the  $\nu$ SMEFT and explicit relations between operators linked by equations of motion; *(ii)* a complete basis for the low-energy effective field theory ( $\nu$ LEFT) and the tree-level matching onto the  $\nu$ SMEFT; *(iii)* partial one-loop anomalous dimensions in the  $\nu$ LEFT. This way, our work comprises a new step forward towards the systematisation of one-loop computations in effective field theories, especially if the SM neutrinos are Dirac.

# Contents

<b>1</b>	<b>Introduction</b>	<b>2</b>
<b>2</b>	<b>Model and effective description</b>	<b>4</b>
<b>3</b>	<b>Matching</b>	<b>7</b>
<b>4</b>	<b>Sterile neutrino phenomenology</b>	<b>13</b>
<b>5</b>	<b>Conclusions</b>	<b>15</b>
<b>A</b>	<b>Mathematical tools</b>	<b>16</b>
<b>B</b>	<b>Details of computation of the UV amplitudes</b>	<b>17</b>
B.1	Amplitude for one $B$ and no Higgs bosons . . . . .	17
B.2	Amplitude for one Higgs and no gauge bosons . . . . .	18
B.3	Amplitude for one Higgs and one photon . . . . .	18
B.4	Amplitude for one Higgs and one $W$ . . . . .	20
B.5	Amplitude for two Higgses and no gauge bosons . . . . .	20
B.6	Amplitude for two Higgses and one $W^3$ . . . . .	21
B.7	Amplitude for three Higgses and no gauge bosons . . . . .	21
B.8	Amplitude for four $N$ fermions . . . . .	22
B.9	Amplitude for two $N$ fermions and two neutrinos . . . . .	22
B.10	Amplitude for six Higgses . . . . .	23
<b>C</b>	<b>Matching the <math>\nu</math>SMEFT onto the <math>\nu</math>LEFT and anomalous dimensions</b>	<b>23</b>

## 1 Introduction

Effective field theories (EFTs) are being used to describe the effects of new heavy particles at low energy in terms of operators of dimension higher than four. A well acknowledged advantage of this approach is its generality. The only model dependence resides in the light degrees of freedom out of which the EFT is built. (The symmetries of the EFT are in principle also debatable, but by now the group of gauge symmetries  $SU(3)_c \times SU(2)_L \times U(1)_Y$  is well established.) Among other aspects, this choice depends crucially on the nature of neutrinos. If neutrinos are Majorana, the simplest assumption is that the infrared (IR) comprises only the Standard Model (SM) fields. The resulting EFT,

known as SMEFT [1, 2], has been extensively studied in the recent years; see Ref. [3] for a fresh review. If neutrinos are Dirac, the low-energy sector has to be extended with right-handed (RH) singlet fermions. The corresponding EFT is referred to as  $\nu$ SMEFT [4, 5]. It has also been applied to the case in which the new RH neutrinos are themselves Majorana, as predicted in numerous models. With the same spirit, other EFTs have considered also new scalars in the IR; see *e.g.* Refs. [6–8].

A common feature of all these EFTs is that they predict new processes that are completely absent in the renormalisable SM. Many of these processes have not been studied yet experimentally. These include, among others, rare decays of the top quark such as  $t \rightarrow \ell^+ \ell^- j$  [9, 10],  $t \rightarrow b \bar{b} j$  [10, 11] or the non-resonant  $t \rightarrow b \ell^+ + E_T^{\text{miss}}$  [12] as well as rare decays of the Higgs boson including  $h \rightarrow \ell^+ \ell^- + 4j$  [13],  $h \rightarrow \gamma(\gamma) + E_T^{\text{miss}}$  [14]. However, this bottom-up approach is not without drawbacks. Most importantly, operators other than those triggering the signals of interest are generally also present (with correlated coefficients) in concrete ultraviolet (UV) models; some of them being very constrained. Likewise, it is hard to prioritise one search over others.

It is therefore desirable that searches motivated by pure EFT inspection are also supported by realistic UV models <sup>1</sup>. This exercise requires matching UV models to the EFT, generally at one loop (at which several of the most interesting and/or dangerous operators appear often). In the usual diagrammatic approach, this process consists of computing tens of one-light-particle-irreducible off-shell amplitudes in both the UV and the EFT. This is a very demanding task that in turn requires knowledge of a full off-shell basis of EFT operators (only those linked by algebraic identities and integration by parts being removed) and their relations by equations of motion. If low energy ( $E \ll v$ , with  $v \sim 246$  GeV being the Higgs vacuum expectation value) observables are to be computed, then the corresponding EFT in the electroweak (EW) symmetry broken phase must be also known, as well as its matching to the aforementioned operators. Renormalisation group evolution (RGE) of the Wilson coefficients in both EFTs might be also needed.

While several of these points have been already addressed in the SMEFT <sup>2</sup>, very little is known about the  $\nu$ SMEFT beyond a full (on-shell) basis of up to dimension-seven operators [4, 5, 21, 22]. Moreover, while new techniques [23–28] and tools [29–31] for one-loop matching are also being developed, a severe obstacle for progress in this respect is

---

<sup>1</sup>We are well aware that “realistic” is an arguable concept. Here we adopt the notion that a “realistic” UV model should involve less free parameters than the EFT (which in turn restricts the number of new independent heavy fields), and that there should not be large cancellations between different couplings of similar size.

<sup>2</sup>The first complete set of dimension-six operators was obtained in Ref. [1]. Several of them were shown to be related by equations of motion in Ref. [2]. The corresponding EFT after EW symmetry breaking (EWSB), known as LEFT, was worked out in Ref. [15]; the tree-level matching of the SMEFT onto the LEFT was also provided in the same article. This computation has been recently performed at one loop in Ref. [16]. Finally, the RGE of the SMEFT and LEFT operators was presented in Refs. [17–19] and Ref. [20], respectively.

precisely the lack of explicit one-loop matching computations to which compare to in the literature [31]. (To the best of our knowledge, partial examples of one-loop matching have been only provided for the SM extended with a real scalar singlet [28,32,33], with a charged scalar singlet [34], with some colourless EW multiplets for very particular parameters [23] and with a vector-like quark singlet [29].)

In light of the discussion above, in this paper we consider a simple UV model whose EFT description is the  $\nu$ SMEFT, for which we provide a full off-shell basis and relations between different operators by equations of motion; see Section 2. In Section 3 we perform the actual one-loop matching using the diagrammatic approach. We provide mathematical tools used and details of loop computations in Appendices A and B, respectively. In Section 4 we study the phenomenology of the resulting EFT (with operators with correlated Wilson coefficients, as they depend on only a very small number of UV couplings), both in the Majorana and in the Dirac cases, and highlight the importance of performing new Higgs searches at the LHC. To this aim, we also rely on a full on-shell basis of the EFT after EWSB and its matching onto the  $\nu$ SMEFT, as well as on partial RGE, all of which we provide in Appendix C.

## 2 Model and effective description

We consider the SM extended with a light RH fermionic singlet  $N$ , as well as two heavy vector-like fermions  $X_E \sim (\mathbf{1}, \mathbf{2})_{1/2}$ ,  $X_N \sim (\mathbf{1}, \mathbf{1})_1$  and a heavy singly-charged scalar  $\varphi \sim (\mathbf{1}, \mathbf{1})_{-1}$ . The numbers within parentheses and the subindex indicate the representations of  $(SU(3)_c, SU(2)_L)$  and the hypercharge  $Y$ , respectively. We assume CP and baryon number conservation, while lepton number and lepton flavour conservation are only broken by the small (potentially vanishing)  $N$  mass;  $N$  is assumed to couple only to the electron (or to the muon; this choice does not alter our phenomenological results). Moreover, we assume that the heavy fields are odd under a  $\mathbb{Z}_2$  symmetry under which all SM fields as well as  $N$  are even.

We denote by  $e, u, d$  the RH leptons and quarks; and by  $L, Q$  the left-handed counterparts. We name the gluon and the EW gauge bosons by  $G$  and  $W, B$ , respectively. Let us call the Higgs doublet by  $H = [G^+, (h + iG^0)/\sqrt{2}]$  and  $\tilde{H} = i\sigma_2 H^*$ , with  $\sigma_I, I = 1, 2, 3$ , being the Pauli matrices. The Lagrangian of this model reads:

$$\mathcal{L} = \mathcal{L}_{SM+N} + \mathcal{L}_{\text{heavy}} , \quad (2.1)$$

with

$$\begin{aligned} \mathcal{L}_{SM+N} = & -\frac{1}{4}G_{\mu\nu}^A G^{A\mu\nu} - \frac{1}{4}W_{\mu\nu}^I W^{I\mu\nu} - \frac{1}{4}B_{\mu\nu} B^{\mu\nu} \\ & + (D_\mu H)^\dagger (D^\mu H) + \mu_H^2 H^\dagger H - \frac{1}{2}\lambda_H (H^\dagger H)^2 \end{aligned}$$

$$\begin{aligned}
& + i (\bar{Q}\not{D}Q + \bar{u}\not{D}u + \bar{d}\not{D}d + \bar{L}\not{D}L + \bar{e}\not{D}e + \bar{N}\not{D}N) \\
& + \left[ m_N \bar{N}^c N - \bar{Q} Y_d H d - \bar{Q} Y_u \tilde{H} u - \bar{L} Y_e H e - \bar{L} Y_N \tilde{H} N + \text{h.c.} \right], \quad (2.2)
\end{aligned}$$

and

$$\begin{aligned}
\mathcal{L}_{\text{heavy}} = & \overline{X_E} (i\not{D} - M_{X_E}) X_E + \overline{X_N} (i\not{D} - M_{X_N}) X_N \\
& + (D_\mu \varphi)^* (D^\mu \varphi) - M_\varphi^2 \varphi^* \varphi - \lambda_{\varphi\varphi} (\varphi^* \varphi)^2 - \lambda_{\varphi H} (\varphi^* \varphi) (H^\dagger H) \\
& + \left[ g_X \overline{X_E} \tilde{H} X_N + g_L \overline{X_E} \varphi^* L + g_N \overline{X_N} \varphi^* N + \text{h.c.} \right]. \quad (2.3)
\end{aligned}$$

Our conventions for the covariant derivative of a colour singlet field  $\phi$  and for the EW field strength tensors are

$$D_\mu \phi = (\partial_\mu - igT^I W_\mu^I - ig'Y B_\mu) \phi, \quad (2.4)$$

$$W_{\mu\nu}^I = \partial_\mu W_\nu^I - \partial_\nu W_\mu^I + g\varepsilon^{IJK} W_\mu^J W_\nu^K, \quad B_{\mu\nu} = \partial_\mu B_\nu - \partial_\nu B_\mu, \quad (2.5)$$

where  $T_I = \sigma_I/2$  are the  $SU(2)$  generators.

This model features a number of interesting properties. *(i)* If the heavy particles are integrated out, no effective operators arise at tree level. *(ii)* Because of this, in the IR only tree-level amplitudes are to be computed while matching at one loop<sup>3</sup>. *(iii)* For the very same reason, UV corrections to light field propagators can be neglected [29]. *(iv)* Likewise, for all practical purposes in the process of matching, any heavy renormalised mass  $M$  (evaluated at a scale  $\mu$  equal to the physical mass) can be identified with the physical mass itself. Finally, for  $m_N \neq 0$ , this model features also the decay  $N \rightarrow \nu\gamma$ . Any other model fulfilling the aforementioned properties necessarily involves a larger number of degrees of freedom.

At energies  $E < M \equiv \min\{M_{X_E}, M_{X_N}, M_\varphi\}$ , this model can be described by a local EFT built upon the SM fields and  $N$ , also known as  $\nu\text{SMEFT}$ . To leading order in the expansion in  $E/M$ , it is given by  $\mathcal{L}_{SM+N}$  (with IR parameters) and a set of dimension-six operators. A basis of such operators<sup>4</sup>, obtained with the help of **BasisGen** [35]

<sup>3</sup>Indeed, any one-loop amplitude in the UV and in the EFT would read  $\mathcal{M}_{UV} \sim g_{UV}/(4\pi)^2$  and  $\mathcal{M}_{EFT} \sim \alpha_{EFT}[1 + g_{EFT}/(4\pi)^2]$ , respectively. Matching  $\mathcal{M}_{UV} = \mathcal{M}_{EFT}$  implies therefore

$$\alpha_{EFT} \sim \frac{g_{UV}}{(4\pi)^2} \left[ 1 - \frac{g_{EFT}}{(4\pi)^2} \right] = \frac{g_{UV}}{(4\pi)^2} + \mathcal{O} \left\{ \frac{1}{(4\pi)^4} \right\}.$$

The last term in the right-hand side of the equation is formally of the same order as two-loop corrections and hence negligible.

<sup>4</sup>We are not showing explicitly the CP counterparts of these operators, because we assume CP conservation. However, they include:  $iB_{\mu\nu}(\bar{N}\gamma^\mu\partial^\nu N)$  (the one without  $i$ , for both the normal field strength and for the dual, is redundant),  $i\mathcal{O}_{NB}$ ,  $i\mathcal{O}_{NW}$ , (dipole operators with the dual are redundant),  $i\mathcal{O}_{LN}^{1,2,3,4}$ ,  $i\mathcal{O}_{LNH}$ ,  $i\mathcal{O}_{HN}$  ( $i\mathcal{O}_{NN}^2$  is redundant) and  $i\mathcal{O}_{HN e}$ . Note that  $\partial^\nu \tilde{B}_{\mu\nu}(\bar{N}\gamma^\mu N)$  vanishes due to the Bianchi identity. On the four-fermion side, we would have  $i\mathcal{O}_{duNe}$ ,  $i\mathcal{O}_{LNLe}$ ,  $i\mathcal{O}_{LNQd}$ ,  $i\mathcal{O}_{LdQN}$  and  $i\mathcal{O}_{QuNL}$ .

0-Higgs	1-Higgs	2-Higgs
$\mathcal{O}_{DN}^1 = \bar{N}\partial^2\phi N$	$\mathcal{O}_{NB} = \bar{L}\sigma^{\mu\nu}N\tilde{H}B_{\mu\nu}$ , $\mathcal{O}_{NW} = \bar{L}\sigma^{\mu\nu}N\sigma_I\tilde{H}W_{\mu\nu}^I$	$\mathcal{O}_{HN} = \bar{N}\gamma^\mu N(H^\dagger iD_\mu H)$
$\mathcal{O}_{DN}^2 = i\tilde{B}_{\mu\nu}(\bar{N}\gamma^\mu\partial^\nu N)$	$\mathcal{O}_{LN}^1 = \bar{L}ND^2\tilde{H}$ , $\mathcal{O}_{LN}^2 = \bar{L}\partial_\mu ND^\mu\tilde{H}$	$\mathcal{O}_{NN}^2 = \bar{N}i\phi N(H^\dagger H)$
$\mathcal{O}_{DN}^3 = \partial^\nu B_{\mu\nu}(\bar{N}\gamma^\mu N)$	$\mathcal{O}_{LN}^3 = i\bar{L}\sigma^{\mu\nu}\partial_\mu ND_\nu\tilde{H}$ , $\mathcal{O}_{LN}^4 = \bar{L}(\partial^2 N)\tilde{H}$	$\mathcal{O}_{HNe} = \bar{N}\gamma^\mu e(\tilde{H}^\dagger iD_\mu H)$
3-Higgs: $\mathcal{O}_{LNH} = \bar{L}\tilde{H}N(H^\dagger H)$		

Table 1: *Relevant bosonic operators. The h.c. is implied when needed. For example,  $\mathcal{O}_{DN}^1 = \bar{N}\partial^2\phi N + h.c.$ ; therefore all Wilson coefficients are real.*

RRRR	$\mathcal{O}_{NN} = (\bar{N}\gamma_\mu N)(\bar{N}\gamma^\mu N)$	
	$\mathcal{O}_{eN} = (\bar{e}\gamma_\mu e)(\bar{N}\gamma^\mu N)$	$\mathcal{O}_{uN} = (\bar{u}\gamma_\mu u)(\bar{N}\gamma^\mu N)$
	$\mathcal{O}_{dN} = (\bar{d}\gamma_\mu d)(\bar{N}\gamma^\mu N)$	$\mathcal{O}_{duNe} = (\bar{d}\gamma_\mu u)(\bar{N}\gamma^\mu e)$
LLRR	$\mathcal{O}_{LN} = (\bar{L}\gamma_\mu L)(\bar{N}\gamma^\mu N)$	$\mathcal{O}_{QN} = (\bar{Q}\gamma_\mu Q)(\bar{N}\gamma^\mu N)$
LRRL	$\mathcal{O}_{LNLe} = (\bar{L}N)\epsilon(\bar{L}e)$	$\mathcal{O}_{LNQd} = (\bar{L}N)\epsilon(\bar{Q}d)$
	$\mathcal{O}_{LdQN} = (\bar{L}d)\epsilon(\bar{Q}N)$	$\mathcal{O}_{QuNL} = (\bar{Q}u)(\bar{N}L)$

Table 2: *Relevant four-fermion operators.*

(see Ref. [36] for a similar code), is given in Tabs. 1 and 2. The operators in grey are redundant *only* when evaluated on shell. (Redundancies due to algebraic or Fierz identities or integration by parts have been removed.) Indeed, neglecting the small  $m_N$  and the Yukawa couplings, the relevant equations of motion of  $\mathcal{L}_{SM+N}$  read:

$$i\phi N = 0, \quad (2.6)$$

$$(D^2\tilde{H})^i = \mu_H^2\tilde{H}^i - \lambda_H(H^\dagger H)\tilde{H}^i, \quad (2.7)$$

$$\partial^\nu B_{\nu\mu} = -\frac{g'}{2}(iH^\dagger D_\mu H + h.c.) - g'Y^f\bar{f}\gamma_\mu f, \quad (2.8)$$

where  $f$  runs over all  $SM + N$  fermions. (The top Yukawa coupling is not negligible; however, its only impact would be the generation of four-fermion operators involving top quarks and  $N$ , for which there are no sensible searches.) As a consequence, the following relations hold on shell for the operators in grey:

$$\mathcal{O}_{DN}^1 = 0, \quad (2.9)$$

$$\mathcal{O}_{DN}^2 = -\mathcal{O}_{DN}^3, \quad (2.10)$$

$$\mathcal{O}_{DN}^3 = \frac{g'}{2}\mathcal{O}_{HN} + g'Y^f\mathcal{O}_{fN}, \quad (2.11)$$

$$\mathcal{O}_{LN}^1 = \left( \mu_H^2 \bar{L} \tilde{H} N + \text{h.c.} \right) - \lambda_H \mathcal{O}_{LNH}, \quad (2.12)$$

$$\mathcal{O}_{LN}^2 = -\mathcal{O}_{LN}^3, \quad (2.13)$$

$$\mathcal{O}_{LN}^3 = \left( \frac{\mu_H^2}{2} \bar{L} \tilde{H} N + \text{h.c.} \right) - \frac{\lambda_H}{2} \mathcal{O}_{LNH} + \frac{g'}{8} \mathcal{O}_{NB} - \frac{g}{8} \mathcal{O}_{NW}, \quad (2.14)$$

$$\mathcal{O}_{LN}^4 = 0, \quad (2.15)$$

$$\mathcal{O}_{NN}^2 = 0. \quad (2.16)$$

As a final remark, let us note that, in light of these equations, effective operators involving  $N$  do not generate any purely SMEFT operators upon using the equations of motion.

### 3 Matching

Hereafter, we assume for simplicity  $M_{X_E} = M_{X_N} = M_\varphi = M$ . Also, we focus on the regime  $g_X \sim g_L \sim \lambda_{\varphi H} \ll g_N$ , and  $g_N > 1$ . This way, the mass and loop suppression in operators involving  $N$  is compensated by the large  $g_N$ . On the other hand, purely SMEFT operators can be neglected; the only exception being the operator  $\mathcal{O}_6 = (H^\dagger H)^3$  because of the large combinatorial enhancement.

Our process of matching consists of equating one-light-particle-irreducible amplitudes computed in both the UV and the EFT at a scale  $\mu = M$  in  $\overline{MS}$  with space-time dimension  $d = 4 - 2\epsilon$ . Following the discussion above, we only compute those amplitudes involving  $N$  (and the one with six Higgses). Let us also note that, by virtue of Eq. 2.9, the amplitude involving just two  $N$  fields, to which only this operator contributes, does not need to be computed. Likewise, due to the absence of heavy particle couplings to  $e$  in the UV Lagrangian, it can be trivially seen that  $\alpha_{HN_e} = 0$ .

The operators  $\mathcal{O}_{DN}^2$  and  $\mathcal{O}_{DN}^3$  can be matched by computing the amplitude given by the diagrams <sup>5</sup> (a) and (b) in Fig. 1. We use the momentum of the incoming  $N$  and the momentum of the  $B$ ,  $p_N$  and  $p_B$ , respectively. In  $\overline{MS}$  we drop terms proportional to  $(1/\epsilon + \log 4\pi - \gamma)$ , where  $\gamma$  is the Euler-Mascheroni constant. The amplitudes in the UV and in the EFT to order  $\mathcal{O}(p^2)$  read:

$$i\mathcal{M}_{UV} = \frac{ig'g_N^2}{96\pi^2 M^2} \bar{u}(p_N - p_B) P_L \left[ \gamma^\mu \left( p_B^2 - p_B p_N + \not{p}_B \not{p}_N \right) - p_B^\mu \not{p}_B - p_B^\mu \not{p}_N + p_N^\mu \not{p}_B \right] u(p_N) \epsilon_\mu^*(p_B), \quad (3.1)$$

---

<sup>5</sup>All Feynman diagrams in this article are produced with the `TikZ-Feynman` package [37].

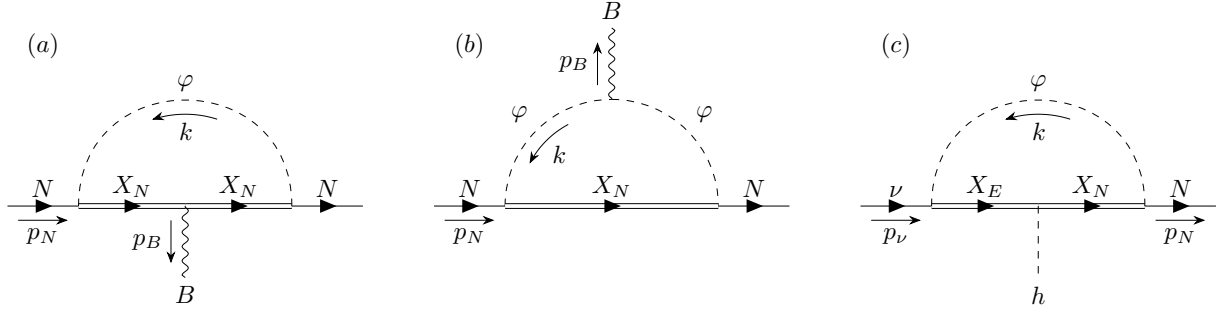


Figure 1: (a) and (b) Diagrams for the amplitude  $\langle NNB \rangle$  in the UV, to which  $\mathcal{O}_{DN}^2$  and  $\mathcal{O}_{DN}^3$  contribute in the IR. (c) Diagram for the amplitude  $\langle \nu Nh \rangle$  in the UV, to which  $\mathcal{O}_{LN}^1$ ,  $\mathcal{O}_{LN}^2$ ,  $\mathcal{O}_{LN}^3$  and  $\mathcal{O}_{LN}^4$  contribute in the IR.

$$\begin{aligned}
i\mathcal{M}_{EFT} = \frac{i}{\Lambda^2} \bar{u}(p_N - p_B) P_L \left[ \gamma^\mu \left( \alpha_{DN}^3 p_B^2 - 2\alpha_{DN}^2 p_B p_N + 2\alpha_{DN}^2 \not{p}_B \not{p}_N \right) \right. \\
\left. - \alpha_{DN}^3 p_B^\mu \not{p}_B - 2\alpha_{DN}^2 p_B^\mu \not{p}_N + 2\alpha_{DN}^2 p_N^\mu \not{p}_B \right] u(p_N) \epsilon_\mu^*(p_B). \quad (3.2)
\end{aligned}$$

We provide all details about the computation of this and the forthcoming UV amplitudes in Appendix B.

The operators  $\mathcal{O}_{LN}^1$ ,  $\mathcal{O}_{LN}^2$ ,  $\mathcal{O}_{LN}^3$  and  $\mathcal{O}_{LN}^4$ , as well as  $Y_N$  in the IR, can be matched by computing the amplitude represented by the diagram (c) in Fig. 1. We take  $p_\nu$  and  $p_N$  as independent momenta. To order  $\mathcal{O}(p^2)$  we have:

$$i\mathcal{M}_{UV} = \frac{ig_N g_X g_L}{96\sqrt{2}\pi^2 M^2} \bar{u}(p_N) P_L \left[ 6M^2 \left( 1 - \log \frac{\mu^2}{M^2} \right) - p_\nu^2 - p_N^2 + p_\nu p_N + \not{p}_N \not{p}_\nu \right] u(p_\nu), \quad (3.3)$$

$$\begin{aligned}
i\mathcal{M}_{EFT} = \frac{i}{\sqrt{2}\Lambda^2} \bar{u}(p_N) P_L \left[ -Y_N \Lambda^2 - \alpha_{LN}^1 p_\nu^2 + (\alpha_{LN}^2 - \alpha_{LN}^1 - \alpha_{LN}^4) p_N^2 \right. \\
\left. + (2\alpha_{LN}^1 - \alpha_{LN}^2 + \alpha_{LN}^3) p_\nu p_N - \alpha_{LN}^3 \not{p}_N \not{p}_\nu \right] u(p_\nu). \quad (3.4)
\end{aligned}$$

The other two operators involving a single Higgs field are  $\mathcal{O}_{NB}$  and  $\mathcal{O}_{NW}$ . They can be matched by computing the amplitude represented by the diagrams in Fig. 2. Taking  $p_\gamma$ ,  $p_h$  and  $p_N$  as independent momenta, the results in the UV and in the EFT up to order  $\mathcal{O}(p)$  read:

$$i\mathcal{M}_{UV} = \frac{ig_L g_X g_N e}{96\sqrt{2}\pi^2 M^2} \bar{u}(p_N) P_L \left[ \gamma^\mu \not{p}_\gamma - p_\gamma^\mu \right] u(p_\nu) \epsilon_\mu^*(p_\gamma), \quad (3.5)$$



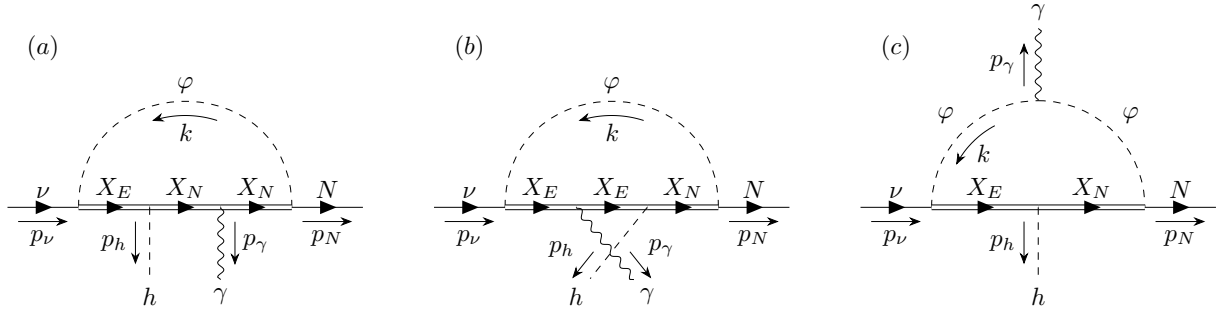


Figure 2: Diagrams for the amplitude  $\langle \nu N h \gamma \rangle$  in the UV, to which  $\mathcal{O}_{NB}$  and  $\mathcal{O}_{NW}$  contribute in the IR.

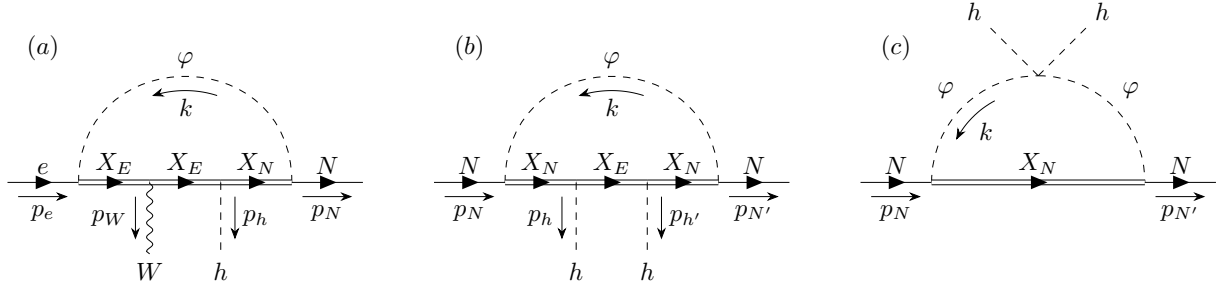


Figure 3: (a) Diagram for the amplitude  $\langle e N W h \rangle$  in the UV, to which  $\mathcal{O}_{LN}^1$ ,  $\mathcal{O}_{LN}^2$ ,  $\mathcal{O}_{LN}^3$  and  $\mathcal{O}_{NW}$  contribute in the IR. (b) and (c) Diagrams for the amplitude  $\langle N N h h \rangle$  in the UV, to which  $\mathcal{O}_{NN}^2$  contributes in the IR. (Note that, despite not explicitly shown, diagram (b) but with the two Higgses exchanged is also present.)

$$i\mathcal{M}_{EFT} = \frac{\sqrt{2}i}{\Lambda^2} (c_W \alpha_{NB} + s_W \alpha_{NW}) \bar{u}(p_N) P_L \left[ \gamma^\mu \not{p}_\gamma - p_\gamma^\mu \right] u(p_\nu) \epsilon_\mu^*(p_\gamma). \quad (3.6)$$

Here  $c_W \equiv \cos \theta_W$  and  $s_W \equiv \sin \theta_W$ , with  $\theta_W$  being the weak mixing angle. (Let us emphasise that in our convention,  $W_\mu^3 = c_W Z_\mu + s_W A_\mu$ ,  $B_\mu = c_W A_\mu - s_W Z_\mu$ .) This amplitude was also computed previously in Ref. [14] (see appendix therein). Still, one more amplitude needs to be computed in order to completely fix the Wilson coefficients of the one-Higgs operators. We choose that represented by the diagram (a) in Fig. 3. Taking  $p_h$ ,  $p_W$  and  $p_N$  as independent momenta, we have to order  $\mathcal{O}(p)$ :

$$i\mathcal{M}_{UV} = \frac{ig_N g_X g_L g}{192\pi^2 M^2} \bar{u}(p_N) P_L \left[ p_N^\mu - 2p_h^\mu - p_W^\mu - \gamma^\mu \not{p}_N \right] u(p_e) \epsilon_\mu^*(p_W), \quad (3.7)$$

$$i\mathcal{M}_{EFT} = \frac{ig}{2\Lambda^2} \bar{u}(p_N) P_L \left[ -(\alpha_{LN}^2 + \alpha_{LN}^3) p_N^\mu - 2\alpha_{LN}^1 p_h^\mu - \left( 4\frac{\alpha_{NW}}{g} + \alpha_{LN}^1 \right) p_W^\mu + \alpha_{LN}^3 \gamma^\mu \not{p}_N + 4\frac{\alpha_{NW}}{g} \gamma^\mu \not{p}_W \right] u(p_e) \epsilon_\mu^*(p_W). \quad (3.8)$$

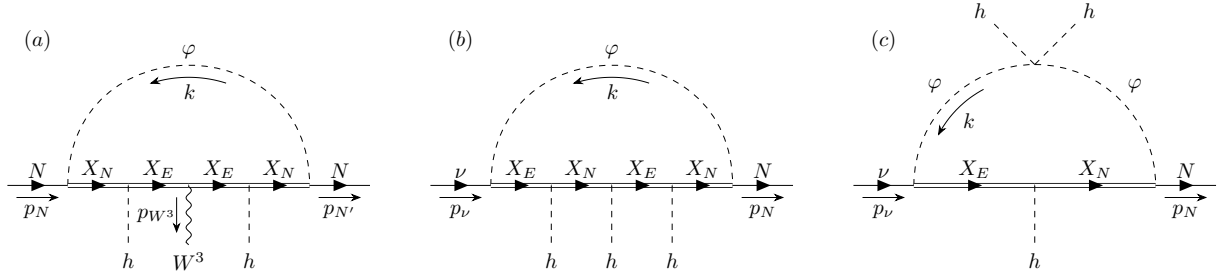


Figure 4: (a) Diagram for the amplitude  $\langle NNW^3hh \rangle$  in the UV, to which the operator  $\mathcal{O}_{HN}$  contributes in the IR. (b) and (c) Diagrams for the amplitude  $\langle \nu Nhhhh \rangle$  in the UV, to which  $\mathcal{O}_{LNH}$  contributes in the IR. (Note that, despite not explicitly shown, all these diagrams but with the corresponding Higgs legs exchanged are also present.)

The operator  $\mathcal{O}_{NN}^2$  can be matched by computing the amplitude represented by the diagrams (b) and (c) in Fig. 3, while the operator  $\mathcal{O}_{HN}$  by computing the diagram (a) in Fig. 4. (It might seem that  $\mathcal{O}_{HN}$  also contributes to the former amplitude; however, only its CP counterpart  $i\mathcal{O}_{HN}$ , which we do not need to consider, does it.) The first one reads, to order  $\mathcal{O}(p)$ :

$$i\mathcal{M}_{UV} = -\frac{ig_N^2\lambda_{\varphi H}}{96\pi^2M^2}\bar{u}(p_{N'})P_L\left[\not{p}_N + \not{p}_{N'}\right]u(p_N), \quad (3.9)$$

$$i\mathcal{M}_{EFT} = \frac{i}{\Lambda^2}\alpha_{NN}^2\bar{u}(p_{N'})P_L\left[\not{p}_N + \not{p}_{N'}\right]u(p_N). \quad (3.10)$$

In the UV and EFT to zero momentum, the second aforementioned amplitude reads:

$$i\mathcal{M}_{UV} = \frac{igg_N^2g_X^2}{96\pi^2M^2}\bar{u}(p_{N'})P_L\gamma^\mu u(p_N)\epsilon_\mu^*(p_{W^3}), \quad (3.11)$$

$$i\mathcal{M}_{EFT} = -\frac{i\alpha_{HN}g}{\Lambda^2}\bar{u}(p_{N'})P_L\gamma^\mu u(p_N)\epsilon_\mu^*(p_{W^3}). \quad (3.12)$$

The operator  $\mathcal{O}_{LNH}$  can be matched by computing the amplitude depicted by the diagrams (b) and (c) in Fig. 4. To zero momentum, the amplitudes in the UV and in the EFT are given by [14]:

$$i\mathcal{M}_{UV} = \frac{ig_Ng_Xg_L}{32\sqrt{2}\pi^2M^2}(\lambda_{\varphi H} - g_X^2)\bar{u}(p_N)P_Lu(p_\nu), \quad (3.13)$$

$$i\mathcal{M}_{EFT} = \frac{3i\alpha_{LNH}}{\sqrt{2}\Lambda^2}\bar{u}(p_N)P_Lu(p_\nu). \quad (3.14)$$

On the side of four-fermion operators, the only such non-vanishing interactions (before using the equations of motion) are  $\mathcal{O}_{NN}$  and  $\mathcal{O}_{LN}$ . They can be matched by computing the amplitudes depicted by the diagrams (a) and (b) in Fig. 5, respectively. The UV and EFT expressions for each amplitude to zero momentum read, respectively:

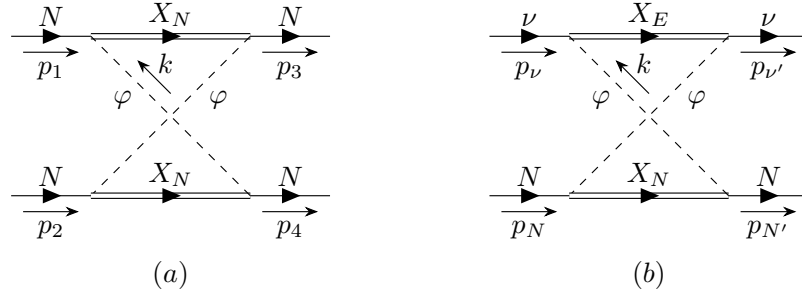


Figure 5: (a) Diagram for the amplitude  $\langle NNNN \rangle$  in the UV, to which  $\mathcal{O}_{NN}$  contributes in the IR. (Note that, despite not explicitly shown, this diagram but with the two outgoing  $N$ s exchanged also exists.) (b) Diagram for the amplitude  $\langle \nu\nu NN \rangle$  in the UV, to which  $\mathcal{O}_{LN}$  contributes in the IR.

$$i\mathcal{M}_{UV} = -\frac{ig_N^4}{96\pi^2 M^2} [\bar{u}(p_3)\gamma^\mu P_R u(p_1)] [\bar{u}(p_4)\gamma_\mu P_R u(p_2)], \quad (3.15)$$

$$i\mathcal{M}_{EFT} = \frac{4i\alpha_{NN}}{\Lambda^2} [\bar{u}(p_3)\gamma^\mu P_R u(p_1)] [\bar{u}(p_4)\gamma_\mu P_R u(p_2)], \quad (3.16)$$

and

$$i\mathcal{M}_{UV} = -\frac{ig_N^2 g_L^2}{192\pi^2 M^2} [\bar{u}(p_{\nu'})\gamma^\mu P_L u(p_\nu)] [\bar{u}(p_{N'})\gamma_\mu P_R u(p_N)], \quad (3.17)$$

$$i\mathcal{M}_{EFT} = \frac{i\alpha_{LN}}{\Lambda^2} [\bar{u}(p_{\nu'})\gamma^\mu P_L u(p_\nu)] [\bar{u}(p_{N'})\gamma_\mu P_R u(p_N)]. \quad (3.18)$$

Finally, the leading term of the operator  $\mathcal{O}_6$  can be matched by computing, to zero momentum, the amplitude given by the diagrams in Fig. 6. It reads:

$$i\mathcal{M}_{UV} = -\frac{3i(4g_X^6 + 5\lambda_{\varphi H}^3)}{16\pi^2 M^2}, \quad (3.19)$$

$$i\mathcal{M}_{EFT} = \frac{90i\alpha_6}{\Lambda^2}. \quad (3.20)$$

Note that, despite not being  $g_N$  enhanced, the UV expression is not as suppressed as those in the previous cases, due to the large number of diagrams entering this amplitude.

By equating all UV amplitudes to their IR counterparts, we end up with 24 equations (including  $\alpha_{HN_e} = 0$ ) for 16 unknowns; the redundancies reflect the gauge symmetries. Neglecting the running from the scale  $\mu = M$  to  $\mu = v$ , the following identities hold off shell at the EW scale (other Wilson coefficients vanish):

$$Y_N^{IR} = Y_N^{UV} - \frac{g_L g_X g_N}{16\pi^2}, \quad (3.21) \quad \frac{\alpha_{DN}^2}{\Lambda^2} = \frac{eg_N^2}{192\pi^2 c_W M^2}, \quad (3.22)$$

$$\frac{\alpha_{DN}^3}{\Lambda^2} = \frac{eg_N^2}{96\pi^2 c_W M^2}, \quad (3.23) \quad \frac{\alpha_{NB}}{\Lambda^2} = \frac{eg_L g_X g_N}{192\pi^2 c_W M^2}, \quad (3.24)$$

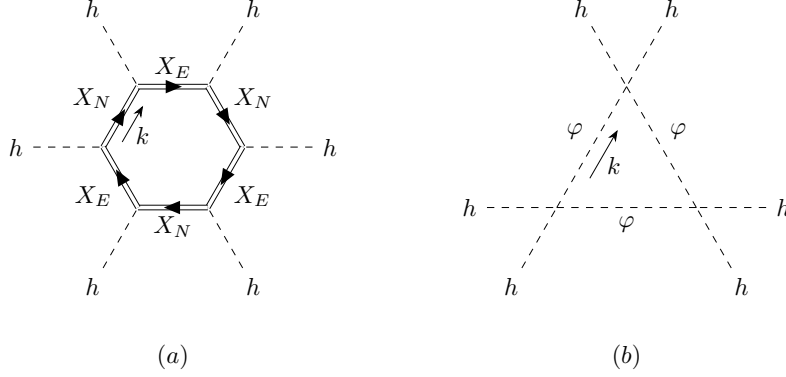


Figure 6: *Diagrams for the amplitude  $\langle hhhhhh \rangle$  in the UV, to which the purely SMEFT operator  $\mathcal{O}_6 = (H^\dagger H)^3$  contributes in the IR. (Note that, despite not explicitly shown, these diagrams but with the corresponding Higgs legs exchanged are also present.)*

$$\frac{\alpha_{LN}^1}{\Lambda^2} = \frac{g_L g_X g_N}{96\pi^2 M^2}, \quad (3.25)$$

$$\frac{\alpha_{HN}}{\Lambda^2} = -\frac{g_X^2 g_N^2}{96\pi^2 M^2}, \quad (3.27)$$

$$\frac{\alpha_{LNH}}{\Lambda^2} = \frac{g_L g_X g_N}{96\pi^2 M^2} (\lambda_{\varphi H} - g_X^2), \quad (3.29)$$

$$\frac{\alpha_{LN}}{\Lambda^2} = -\frac{g_L^2 g_N^2}{192\pi^2 M^2}, \quad (3.31)$$

$$\frac{\alpha_{LN}^3}{\Lambda^2} = -\frac{g_L g_X g_N}{96\pi^2 M^2}, \quad (3.26)$$

$$\frac{\alpha_{NN}^2}{\Lambda^2} = -\frac{\lambda_{\varphi H} g_N^2}{96\pi^2 M^2}, \quad (3.28)$$

$$\frac{\alpha_{NN}}{\Lambda^2} = -\frac{g_N^4}{384\pi^2 M^2}, \quad (3.30)$$

$$\frac{\alpha_6}{\Lambda^2} = -\frac{4g_X^6 + 5\lambda_{\varphi H}^3}{480\pi^2 M^2}, \quad (3.32)$$

where  $e = \sqrt{4\pi\alpha}$ , and  $\alpha \approx 1/137$  stands for the electromagnetic fine-structure constant. Finally, upon using the equations of motion, Eqs. (2.9)–(2.16), the following relations hold on shell (other Wilson coefficients vanish):

$$Y_N^{IR} = Y_N^{UV} - \frac{g_L g_X g_N}{16\pi^2} \left(1 + \frac{m_h^2}{24M^2}\right), \quad (3.33)$$

$$\frac{\alpha_{NW}}{\Lambda^2} = \frac{e g_L g_X g_N}{768\pi^2 s_W M^2}, \quad (3.35)$$

$$\frac{\alpha_{LNH}}{\Lambda^2} = -\frac{g_L g_X g_N}{192\pi^2 M^2} \left[ \frac{m_h^2}{v^2} + 2(g_X^2 - \lambda_{\varphi H}) \right], \quad (3.37)$$

$$\frac{\alpha_{eN}}{\Lambda^2} = -\frac{e^2 g_N^2}{192\pi^2 c_W^2 M^2}, \quad (3.39)$$

$$\frac{\alpha_{QN}}{\Lambda^2} = \frac{e^2 g_N^2}{1152\pi^2 c_W^2 M^2}, \quad (3.41)$$

$$\frac{\alpha_{dN}}{\Lambda^2} = -\frac{e^2 g_N^2}{576\pi^2 c_W^2 M^2}, \quad (3.43)$$

$$\frac{\alpha_{NB}}{\Lambda^2} = \frac{e g_L g_X g_N}{256\pi^2 c_W M^2}, \quad (3.34)$$

$$\frac{\alpha_{HN}}{\Lambda^2} = \frac{g_N^2 (e^2 - 4c_W^2 g_X^2)}{384\pi^2 c_W^2 M^2}, \quad (3.36)$$

$$\frac{\alpha_{LN}}{\Lambda^2} = -\frac{g_N^2 (e^2 + 2c_W^2 g_L^2)}{384\pi^2 c_W^2 M^2}, \quad (3.38)$$

$$\frac{\alpha_{NN}}{\Lambda^2} = -\frac{g_N^4}{384\pi^2 M^2}, \quad (3.40)$$

$$\frac{\alpha_{uN}}{\Lambda^2} = \frac{e^2 g_N^2}{288\pi^2 c_W^2 M^2}, \quad (3.42)$$

$$\frac{\alpha_6}{\Lambda^2} = -\frac{4g_X^6 + 5\lambda_{\varphi H}^3}{480\pi^2 M^2}. \quad (3.44)$$

For convenience, let us also define  $\mathcal{O}_{NA} = c_W \mathcal{O}_{NB} + s_W \mathcal{O}_{NW}$  and  $\mathcal{O}_{NZ} = c_W \mathcal{O}_{NW} - s_W \mathcal{O}_{NB}$ . For the coefficients of these operators we obtain:

$$\frac{\alpha_{NA}}{\Lambda^2} = \frac{eg_L g_X g_N}{192\pi^2 M^2}, \quad (3.45) \quad \frac{\alpha_{NZ}}{\Lambda^2} = \frac{eg_L g_X g_N (1 - 4s_W^2)}{768\pi^2 s_W c_W M^2}. \quad (3.46)$$

## 4 Sterile neutrino phenomenology

In the process of matching we have neglected  $m_N$ . The only effect of  $m_N \neq 0$  would appear in the dimension-five operator  $\overline{N^c} N H^\dagger H$  suppressed not only by the loop factor but also by  $m_N/M$ , namely by  $\sim 10^{-3}$  if  $m_N \sim 1$  GeV and  $M \sim 1$  TeV. (The operator  $\overline{N^c} \sigma^{\mu\nu} N B_{\mu\nu}$  vanishes in this case because  $N$  is Majorana.) However,  $m_N \neq 0$  has a huge impact on the phenomenology of  $N$ , because it allows the latter to decay into  $\nu\gamma$ . The corresponding decay width must be computed after EWSB, namely in the  $\nu$ LEFT, obtained first by matching the  $\nu$ SMEFT at the EW scale and after running down to  $\sim m_N$ . The full list of  $\nu$ LEFT operators involving  $N$  is given in Tab. 3 in Appendix C. The operator that triggers the decay of  $N$  is  $\mathcal{O}_{N\gamma}$ . For completeness, though, we provide tree-level matching of all  $\nu$ SMEFT operators to all  $\nu$ LEFT ones in Eqs. (C.1)–(C.24). The one-loop running of all  $\nu$ LEFT operators generated in our setup, including  $\mathcal{O}_{N\gamma}$ , is also given in the same appendix. Altogether, we have:

$$\Gamma(N \rightarrow \nu\gamma) \approx \frac{m_N^3 \alpha_{N\gamma}^2(v)}{2\pi v^2} \left(1 - \frac{5e^2}{9\pi^2} \log \frac{v}{m_N}\right)^2. \quad (4.1)$$

For simplicity, let us fix  $Y_N^{UV}$  such that  $Y_N^{IR} = \alpha_{LNH} v^2 / (2\Lambda^2)$ ; see Eq. (3.33). This way, the mixing between  $N$  and  $\nu$  vanishes strictly. (Note that the sole important effect of this mixing would be inducing a Majorana neutrino dipole moment for  $\nu$ ; this vanishes however in our case due to lepton flavour conservation [14].)

Different experiments constrain the parameter space under study. The relevant observables can be all computed directly in the  $\nu$ SMEFT. (In quoting the following bounds we have set  $\Lambda = 1$  TeV.) We have first  $\mathcal{B}(Z \rightarrow \nu\nu\gamma\gamma)$ . Experimentally it is bounded to be  $< 3.1 \times 10^{-6}$  [38]. In our context this branching ratio is given by (note that for  $m_N \sim 1$  GeV,  $\mathcal{B}(N \rightarrow \nu\gamma) \approx 1$  [39]):

$$\begin{aligned} \mathcal{B}(Z \rightarrow \nu\nu\gamma\gamma) \approx \mathcal{B}(Z \rightarrow NN) &\approx \frac{1}{\Gamma_Z^{SM}} \frac{m_Z^3 v^2}{24\pi\Lambda^4} \alpha_{HN}^2 \\ &\approx 2.7 \times 10^{-10} g_N^4 (0.029 - g_X^2)^2 \frac{\text{TeV}^4}{M^4}, \end{aligned} \quad (4.2)$$

with  $\Gamma_Z^{SM} \approx 2.5$  GeV. This bound implies in turn a limit on  $\alpha_{HN} < 0.11$ , which is ultimately the most stringent constrain on  $(M, g_N)$ . Other subleading constraints include:

(i)  $\mathcal{B}(Z \rightarrow \nu\nu\gamma)$ , experimentally bounded to be  $< 3.2 \times 10^{-6}$  [40], which implies  $\alpha_{NZ} < 0.081$ ; (ii) the measurement of the total  $W$  boson width,  $\Gamma_W^{\text{total}} = 2.085 \pm 0.042$  GeV, which however does not constrain  $\alpha_{HNe}$  more than a theoretical perturbativity bound implying  $\alpha_{HNe} < 4\pi$ ; (iii) the bound on  $\alpha_{NA} < 0.88$  [14] as obtained from LHC searches for events with one photon and missing energy [41]. (Bounds on  $\alpha_{NA}$  obtained from the study of differential Drell-Yan distributions at the LHC, mediated by both neutral and charged currents, using **Contur** [42] are weaker [14].) The bound on  $\alpha_{NA}$  can be improved to  $\alpha_{NA} < 0.36$  by searches for  $h \rightarrow \gamma\gamma + E_T^{\text{miss}}$ , as proposed in Ref. [14]. This value, however, still leads to a very weak constrain on  $(M, g_N)$ .

The sensitivity to this model via exploration of the operator  $\mathcal{O}_6$  is very limited despite its larger size, even at future facilities. Indeed, the FCC-ee could exclude  $\alpha_6 > 1.9$ , while gravitational wave observatories such as LISA would only probe  $\alpha_6 > 2.8$  [43]. Four-fermion interactions could be bounded at the LHC in searches for  $pp \rightarrow \ell\gamma + E_T^{\text{miss}}$ . However, we are not aware of any such search; a preliminary phenomenological study has been provided in Ref. [44]. Interestingly though, it has been shown that searches for Higgs decaying to a single photon and missing energy could test  $\mathcal{B}(h \rightarrow \nu N) > 1.2 \times 10^{-4}$  [14]. Noticing that

$$\begin{aligned} \mathcal{B}(h \rightarrow \nu N) &\approx \frac{1}{\Gamma_h^{\text{SM}}} \frac{m_h v^4}{16\pi\Lambda^4} \alpha_{LNH}^2 \\ &\approx 2.5 \times 10^{-6} (g_L g_N g_X)^2 (0.13 + g_X^2 - \lambda_{\varphi H})^2 \frac{\text{TeV}^4}{M^4}, \end{aligned} \quad (4.3)$$

with  $\Gamma_h^{\text{SM}} \approx 4$  MeV, the corresponding limit on  $\alpha_{LNH}$  reads  $\alpha_{LNH} < 7.3 \times 10^{-3}$ . We show in Fig. 7 that, when translated to the plane  $(M, g_N)$ , this signal overcomes often the constraint from  $\alpha_{HN}$ .

If lepton number is exactly conserved, *i.e.* in particular,  $m_N = 0$ ,  $N$  is just the RH component of the SM neutrino, which would be Dirac. In this case, the very stringent bounds on the neutrino dipole moment [45] can be only satisfied if  $g_X \approx 0$  (or  $g_L \approx 0$ ). Accordingly, only the operator  $\mathcal{O}_{HN}$  and the four-fermions  $\mathcal{O}_{LN}$ ,  $\mathcal{O}_{eN}$ ,  $\mathcal{O}_{QN}$ ,  $\mathcal{O}_{uN}$  and  $\mathcal{O}_{dN}$  as well as  $\mathcal{O}_{NN}$  could survive, see Eqs. (3.33)–(3.44). ( $\mathcal{O}_6$  can also survive, but we have seen that it is very weakly constrained.) The former enhances the  $Z$  decay into invisible, but the corresponding limit on  $(M, g_N)$  is very weak. Likewise, the bounds on the four-fermion operators involving quarks and charged leptons are of order  $\alpha/\Lambda^2 \lesssim 1 \text{ TeV}^{-2}$  [12], and therefore they are not stringent in this setup in which all operators arise at loop level, and hence the effective scale  $\Lambda$  is rather  $\Lambda \sim 4\pi M$ .

Finally, we are not aware of any significant bound on  $\mathcal{O}_{NN}$ . As things stand, this scenario is very much unconstrained in light of current data, even for  $M \sim$  few hundreds GeV. (In this respect, let us also emphasise that direct LHC searches for singly charged scalars and vector-like leptons, which are present in our UV model, do not constrain this range of masses [46–49].)

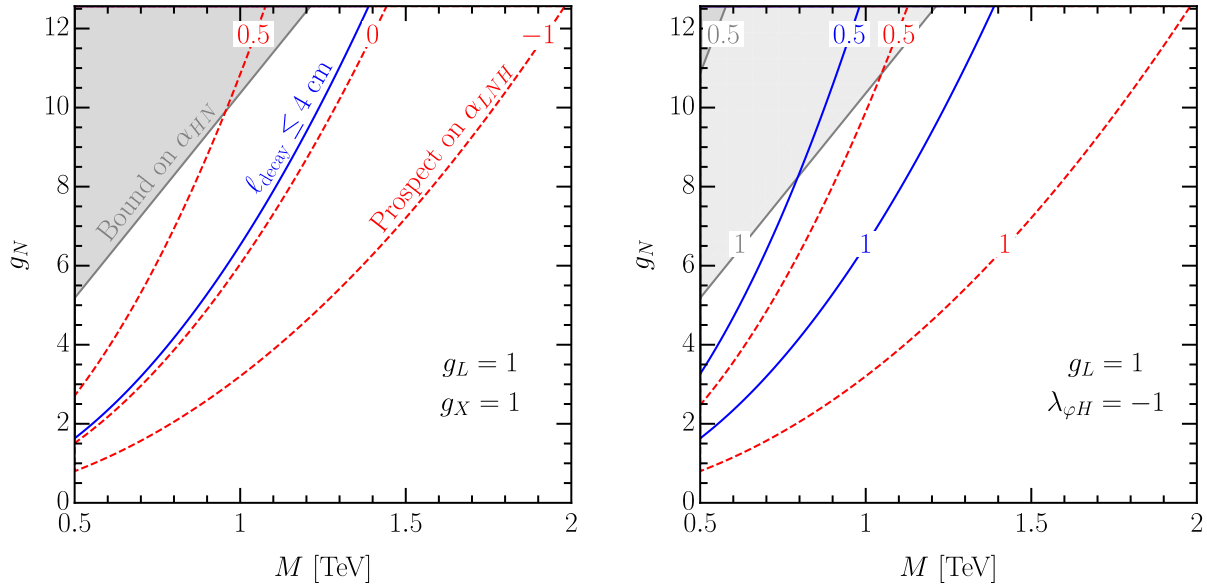


Figure 7: Constraints in the plane  $(M, g_N)$  derived from the bounds on the EFT coefficients summarised in the text. In the region above the blue line,  $N$  with  $m_N = 1$  GeV decays within 4 cm. The actual bound on  $\alpha_{HN}$  from  $Z \rightarrow \nu\nu\gamma\gamma$  and the prospective bound on  $\alpha_{LNH}$  from the  $h \rightarrow \gamma + E_T^{miss}$  analysis proposed in Ref. [14] have been translated to the constraints in the plane  $(M, g_N)$  assuming  $g_X = 1$  and  $\lambda_{\phi H} = -1, 0$  and  $0.5$  (left) as well as  $\lambda_{\phi H} = -1$  and  $g_X = 0.5$  and  $1$  (right).

## 5 Conclusions

In this paper, we have considered a very simple extension of the SM involving a light RH neutrino  $N$  (which can be well the RH part of any of the SM neutrinos if they are Dirac, or a new Majorana neutrino), two heavy fermionic fields and one heavy scalar field, all of them colourless. In the IR, this theory can be described by the  $\nu$ SMEFT. We have shown that, if  $N$  is Majorana, new Higgs decays not yet studied experimentally at the LHC can test this model better than other studies already performed at low-energy facilities; most importantly, searches for  $Z \rightarrow \nu\nu\gamma\gamma$ .

We note that, although this observation is relatively straightforward in the generic EFT, because constrained operators can be set to zero independently of those triggering the signal of interest, this is highly non-trivial in the EFT obtained in this model, in which all Wilson coefficients depend on solely four arbitrary couplings. The fact that the signal of interest is not in conflict with the present constraints in such a simple UV completion of the  $\nu$ SMEFT, strengthens the motivation for novel searches in the Higgs sector.

We have provided a complete calculation of one-loop matching in the diagrammatic approach, obtained upon computing the same one-light-particle-irreducible off-shell am-

plitudes in the UV and in the IR. This complements the very few examples of one-loop matching in the literature, and it is expected that our results will allow faster progress in the automation of tools in this respect [29, 30]. As a byproduct of this work, we have also obtained a complete (off-shell) basis in the  $\nu$ SMEFT, the tree-level matching of the  $\nu$ SMEFT onto the low-energy version (in which the top quark, the Higgs and the  $W$  and  $Z$  bosons are integrated out), that we dubbed  $\nu$ LEFT; as well as some one-loop anomalous dimensions in the latter EFT. We leave the computation of the full RGE anomalous dimension matrix in the  $\nu$ LEFT and in the  $\nu$ SMEFT for future work.

## Acknowledgements

We are grateful to Jose Santiago for helpful discussions. MC is supported by the Spanish MINECO under the Juan de la Cierva programme.

## A Mathematical tools

We have used the following master integrals:

$$\int \frac{d^d k}{(2\pi)^d} \frac{1}{(k^2 - M^2)^n} = \frac{(-1)^n i \Gamma(n - d/2)}{(4\pi)^{d/2} \Gamma(n)} \frac{1}{M^{2n-d}} = A_n, \quad (\text{A.1})$$

$$\int \frac{d^d k}{(2\pi)^d} \frac{k^\mu k^\nu}{(k^2 - M^2)^n} = \underbrace{\frac{1}{2} \frac{(-1)^{n-1} i \Gamma(n - d/2 - 1)}{(4\pi)^{d/2} \Gamma(n)} \frac{1}{M^{2n-d-2}}}_{B_n} g^{\mu\nu}, \quad (\text{A.2})$$

$$\int \frac{d^d k}{(2\pi)^d} \frac{k^\mu k^\nu k^\rho k^\sigma}{(k^2 - M^2)^n} = \underbrace{\frac{1}{4} \frac{(-1)^n i \Gamma(n - d/2 - 2)}{(4\pi)^{d/2} \Gamma(n)} \frac{1}{M^{2n-d-4}}}_{C_n} \times (g^{\mu\nu} g^{\rho\sigma} + g^{\mu\rho} g^{\nu\sigma} + g^{\mu\sigma} g^{\nu\rho}). \quad (\text{A.3})$$

Here  $d$  is the space-time dimension. For expansion in an external momentum  $p$  we have:

$$\frac{1}{(k+p)^2 - M^2} = \frac{1}{k^2 - M^2} \left[ 1 - \frac{2kp + p^2}{k^2 - M^2} + \frac{4(kp)^2}{(k^2 - M^2)^2} \right] + \mathcal{O}(p^3). \quad (\text{A.4})$$

Finally, we have also made use of the following algebraic identities:

$$\epsilon^{\mu\sigma\rho\nu} p_{1\rho} p_{2\nu} \gamma_\sigma \gamma_5 = i \left( \gamma^\mu \not{p}_2 \not{p}_1 + p_1^\mu \not{p}_2 - p_2^\mu \not{p}_1 - \gamma^\mu p_1 p_2 \right), \quad (\text{A.5})$$

$$[D_\mu, D_\nu] = -ig'Y B_{\mu\nu} - igT^I W_{\mu\nu}^I. \quad (\text{A.6})$$



## B Details of computation of the UV amplitudes

### B.1 Amplitude for one $B$ and no Higgs bosons

This amplitude in the UV is given by the diagrams (a) and (b) in Fig. 1. We have:

$$\begin{aligned}
i\mathcal{M}_{UV}^a &= -g'g_N^2\bar{u}(p_N - p_B)P_L \left\{ \mu^{4-d} \int \frac{d^d k}{(2\pi)^d} \frac{1}{D^3} (\not{p}_N - \not{p}_B + \not{k} + M)\gamma^\mu(\not{p}_N + \not{k} + M) \right. \\
&\quad \times \left[ 1 - \frac{2(p_N - p_B)k + (p_N - p_B)^2}{D} + \frac{4[k(p_N - p_B)]^2}{D^2} \right] \\
&\quad \times \left[ 1 - \frac{2p_N k + p_N^2}{D} + \frac{4(kp_N)^2}{D^2} \right] \left. \right\} P_R u(p_N)\epsilon_\mu^*(p_B) \\
&= -g'g_N^2\bar{u}(p_N - p_B)P_L \left\{ [\mu^{2\epsilon}(2\epsilon - 2)B_3 + M^2 A_3]\gamma^\mu \right. \\
&\quad + [12B_4 - A_3 - 48C_5 - 2M^2 A_4 + 12M^2 B_5] \gamma^\mu p_N^2 \\
&\quad + [4B_4 - 16C_5 - M^2 A_4 + 4M^2 B_5] \gamma^\mu p_B^2 \\
&\quad + [48C_5 - 8B_4 + 2M^2 A_4 - 12M^2 B_5] \gamma^\mu p_B p_N + [A_3 - 4B_4] \gamma^\mu \not{p}_B \not{p}_N \\
&\quad + [2A_3 - 16B_4 + 48C_5] p_N^\mu \not{p}_N + [16C_5 - 4B_4] p_B^\mu \not{p}_B \\
&\quad + [12B_4 - 2A_3 - 24C_5] p_B^\mu \not{p}_N + [4B_4 - 24C_5] p_N^\mu \not{p}_B \left. \right\} u(p_N)\epsilon_\mu^*(p_B) \\
&= \frac{ig'g_N^2}{192\pi^2 M^2} \bar{u}(p_N - p_B)P_L \left\{ \gamma^\mu \left( 6M^2 \log \frac{\mu^2}{M^2} + p_N^2 + 3p_B^2 - 3p_B p_N + 2\not{p}_B \not{p}_N \right) \right. \\
&\quad \left. + 2p_N^\mu \not{p}_N - 2p_B^\mu \not{p}_B - 3p_B^\mu \not{p}_N + p_N^\mu \not{p}_B \right\} u(p_N)\epsilon_\mu^*(p_B). \tag{B.1}
\end{aligned}$$

Here and in what follows  $D \equiv k^2 - M^2$ . The second diagram leads to

$$\begin{aligned}
i\mathcal{M}_{UV}^b &= -g'g_N^2\bar{u}(p_N - p_B)P_L \left\{ \mu^{4-d} \int \frac{d^d k}{(2\pi)^d} \frac{1}{D^3} (\not{k} + \not{p}_N + M)(2k^\mu + p_B^\mu) \right. \\
&\quad \times \left[ 1 - \frac{2p_N k + p_N^2}{D} + \frac{4(kp_N)^2}{D^2} \right] \\
&\quad \times \left[ 1 - \frac{2p_B k + p_B^2}{D} + \frac{4(kp_B)^2}{D^2} \right] \left. \right\} P_R u(p_N)\epsilon_\mu^*(p_B) \\
&= -g'g_N^2\bar{u}(p_N - p_B)P_L \left\{ 2\mu^{2\epsilon} B_3 \gamma^\mu + [8C_5 - 2B_4] \gamma^\mu p_N^2 + [8C_5 - 2B_4] \gamma^\mu p_B^2 \right. \\
&\quad + 8C_5 \gamma^\mu p_B p_N + [16C_5 - 4B_4] p_N^\mu \not{p}_N + [16C_5 - 2B_4] p_B^\mu \not{p}_B \\
&\quad \left. + [A_3 - 6B_4 + 8C_5] p_B^\mu \not{p}_N + 8C_5 p_N^\mu \not{p}_B \right\} u(p_N)\epsilon_\mu^*(p_B)
\end{aligned}$$

$$\begin{aligned}
&= \frac{ig'g_N^2}{192\pi^2 M^2} \bar{u}(p_N - p_B) P_L \left\{ \gamma^\mu \left( -6M^2 \log \frac{\mu^2}{M^2} - p_N^2 - p_B^2 + p_B p_N \right) \right. \\
&\quad \left. - 2p_N^\mu \not{p}_N + p_B^\mu \not{p}_N + p_N^\mu \not{p}_B \right\} u(p_N) \epsilon_\mu^*(p_B). \tag{B.2}
\end{aligned}$$

Adding the two pieces together:

$$\begin{aligned}
i\mathcal{M}_{UV} &= i\mathcal{M}_{UV}^a + i\mathcal{M}_{UV}^b \\
&= \frac{ig'g_N^2}{96\pi^2 M^2} \bar{u}(p_N - p_B) P_L \left\{ \gamma^\mu \left( p_B^2 - p_B p_N + \not{p}_B \not{p}_N \right) \right. \\
&\quad \left. - p_B^\mu \not{p}_B - p_B^\mu \not{p}_N + p_N^\mu \not{p}_B \right\} u(p_N) \epsilon_\mu^*(p_B). \tag{B.3}
\end{aligned}$$

## B.2 Amplitude for one Higgs and no gauge bosons

This UV amplitude is represented by the diagram (c) in Fig. 1. We have:

$$\begin{aligned}
i\mathcal{M}_{UV} &= -\frac{g_N g_X g_L}{\sqrt{2}} \bar{u}(p_N) P_L \left\{ \mu^{4-d} \int \frac{d^d k}{(2\pi)^d} \frac{1}{D^3} \left( \not{p}_N + \not{k} + M \right) \left( \not{p}_\nu + \not{k} + M \right) \right. \\
&\quad \times \left[ 1 - \frac{2kp_N + p_N^2}{D} + \frac{4(kp_N)^2}{D^2} \right] \\
&\quad \times \left[ 1 - \frac{2kp_\nu + p_\nu^2}{D} + \frac{4(kp_\nu)^2}{D^2} \right] \left. \right\} P_L u(p_\nu) \\
&= -\frac{g_N g_X g_L}{\sqrt{2}} \bar{u}(p_N) P_L \left\{ \mu^{2\epsilon} (4 - 2\epsilon) B_3 + M^2 A_3 \right. \\
&\quad - [6(B_4 - 4C_5) + M^2(A_4 - 4B_5)] (p_\nu^2 + p_N^2) \\
&\quad \left. + 4(6C_5 + M^2 B_5) p_\nu p_N + (A_3 - 4B_4) \not{p}_N \not{p}_\nu \right\} u(p_\nu) \\
&= \frac{ig_N g_X g_L}{96\sqrt{2}\pi^2 M^2} \bar{u}(p_N) P_L \left\{ 6M^2 \left( 1 - \log \frac{\mu^2}{M^2} \right) - p_\nu^2 - p_N^2 + p_\nu p_N + \not{p}_N \not{p}_\nu \right\} u(p_\nu). \tag{B.4}
\end{aligned}$$

## B.3 Amplitude for one Higgs and one photon

The relevant UV diagrams are depicted in Fig. 2. We have:

$$i\mathcal{M}_{UV}^{a+b} = \frac{g_L g_X g_N e}{\sqrt{2}} \bar{u}(p_N) P_L \int \frac{d^4 k}{(2\pi)^4} \frac{1}{D^4} \left( \not{p}_N + \not{k} + M \right) \left[ 1 - \frac{2kp_N}{D} \right]$$

$$\begin{aligned}
& \times \left\{ \gamma^\mu \left( \not{p}_\gamma + \not{p}_N + \not{k} + M \right) \left[ 1 - \frac{2k(p_\gamma + p_N)}{D} \right] \right. \\
& \quad \left. + \left( \not{p}_h + \not{p}_N + \not{k} + M \right) \gamma^\mu \left[ 1 - \frac{2k(p_h + p_N)}{D} \right] \right\} \\
& \times \left( \not{p}_h + \not{p}_\gamma + \not{p}_N + \not{k} + M \right) \left[ 1 - \frac{2k(p_h + p_\gamma + p_N)}{D} \right] \\
& \times P_L u(p_\nu) \epsilon_\mu^*(p_\gamma) \\
& = \frac{g_L g_X g_N e}{\sqrt{2}} \bar{u}(p_N) P_L \left\{ 2 [2B_4 - 12C_5 + M^2 (A_4 - 10B_5)] p_h^\mu \right. \\
& \quad + 4 [B_4 - 12C_5 - 4M^2 B_5] p_\gamma^\mu \\
& \quad + 6 [2B_4 - 12C_5 + M^2 (A_4 - 6B_5)] p_N^\mu \\
& \quad + [2B_4 - 12C_5 + M^2 (A_4 + 2B_5)] \gamma^\mu \not{p}_h \\
& \quad \left. + [2B_4 + 12C_5 + M^2 (3A_4 - 2B_5)] \gamma^\mu \not{p}_\gamma \right\} u(p_\nu) \epsilon_\mu^*(p_\gamma) \\
& = \frac{ig_L g_X g_N e}{96\sqrt{2}\pi^2 M^2} \bar{u}(p_N) P_L \left\{ -p_h^\mu - p_\gamma^\mu + \gamma^\mu \not{p}_h + \gamma^\mu \not{p}_\gamma \right\} u(p_\nu) \epsilon_\mu^*(p_\gamma), \tag{B.5}
\end{aligned}$$

and

$$\begin{aligned}
i\mathcal{M}_{UV}^c & = \frac{g_L g_X g_N e}{\sqrt{2}} \bar{u}(p_N) P_L \left\{ \int \frac{d^4 k}{(2\pi)^4} \frac{1}{D^4} \left( \not{p}_\gamma + \not{p}_N + \not{k} + M \right) \left( \not{p}_h + \not{p}_\gamma + \not{p}_N + \not{k} + M \right) \right. \\
& \quad \times (p_\gamma^\mu + 2k^\mu) \left[ 1 - \frac{2k(p_\gamma + p_N)}{D} \right] \left[ 1 - \frac{2k(p_h + p_\gamma + p_N)}{D} \right] \\
& \quad \left. \times \left[ 1 - \frac{2kp_\gamma}{D} \right] \right\} P_L u(p_\nu) \epsilon_\mu^*(p_\gamma) \\
& = \frac{g_L g_X g_N e}{\sqrt{2}} \bar{u}(p_N) P_L \left\{ -2 [12C_5 + 2M^2 B_5] p_h^\mu + 2B_4 \gamma^\mu \not{p}_h \right. \\
& \quad + [8(B_4 - 9C_5) + M^2 (A_4 - 12B_5)] p_\gamma^\mu \\
& \quad \left. + 4 [B_4 - 12C_5 - 2M^2 B_5] p_N^\mu \right\} u(p_\nu) \epsilon_\mu^*(p_\gamma) \\
& = \frac{ig_L g_X g_N e}{96\sqrt{2}\pi^2 M^2} \bar{u}(p_N) P_L \left\{ p_h^\mu - \gamma^\mu \not{p}_h \right\} u(p_\nu) \epsilon_\mu^*(p_\gamma). \tag{B.6}
\end{aligned}$$

Adding Eqs. (B.5) and (B.6) together, we get:

$$i\mathcal{M}_{UV} = i\mathcal{M}_{UV}^{a+b} + i\mathcal{M}_{UV}^c = \frac{ig_L g_X g_N e}{96\sqrt{2}\pi^2 M^2} \bar{u}(p_N) P_L \left\{ \gamma^\mu \not{p}_\gamma - p_\gamma^\mu \right\} u(p_\nu) \epsilon_\mu^*(p_\gamma). \tag{B.7}$$

## B.4 Amplitude for one Higgs and one $W$

This amplitude in the UV is depicted by the diagram (a) in Fig. 3. We have:

$$\begin{aligned}
i\mathcal{M}_{UV} &= \frac{g_N g_X g_L g}{2} \bar{u}(p_N) P_L \left\{ \int \frac{d^4 k}{(2\pi)^4} \frac{1}{D^4} (\not{p}_N + \not{k} + M) (\not{p}_h + \not{p}_N + \not{k} + M) \gamma^\mu \right. \\
&\quad \times (\not{p}_W + \not{p}_h + \not{p}_N + \not{k} + M) \left[ 1 - \frac{2k p_N}{D} \right] \\
&\quad \times \left[ 1 - \frac{2k(p_h + p_N)}{D} \right] \left[ 1 - \frac{2k(p_W + p_h + p_N)}{D} \right] \left. \right\} \\
&\quad \times P_L u(p_e) \epsilon_\mu^*(p_W) \\
&= \frac{g_N g_X g_L g}{2} \bar{u}(p_N) P_L \left\{ 4M^2 (A_4 - 6B_5) p_N^\mu + [4B_4 + 2M^2 (A_4 - 8B_5)] p_h^\mu \right. \\
&\quad - 8M^2 B_5 p_W^\mu + [6(B_4 - 6C_5) - M^2 (A_4 - 6B_5)] \gamma^\mu \not{p}_N \\
&\quad + 4(B_4 - 6C_5 + M^2 B_5) \gamma^\mu \not{p}_h \\
&\quad \left. + [4(B_4 - 3C_5) + M^2 (A_4 + 2B_5)] \gamma^\mu \not{p}_W \right\} u(p_e) \epsilon_\mu^*(p_W) \\
&= \frac{i g_N g_X g_L g}{192 \pi^2 M^2} \bar{u}(p_N) P_L \left\{ p_N^\mu - 2p_h^\mu - p_W^\mu - \gamma^\mu \not{p}_N \right\} u(p_e) \epsilon_\mu^*(p_W). \tag{B.8}
\end{aligned}$$

## B.5 Amplitude for two Higgses and no gauge bosons

This UV amplitude is given by the diagrams (b) and (c) in Fig. 3. Taking into account possible permutations of  $p_h$  and  $p_{h'}$ , we have:

$$\begin{aligned}
i\mathcal{M}_{UV}^b &= \frac{g_N^2 g_X^2}{2} \bar{u}(p_{N'}) P_L \int \frac{d^4 k}{(2\pi)^4} \frac{1}{D^4} (\not{p}_{N'} + \not{k} + M) \left[ 1 - \frac{2k p_{N'}}{D} \right] \\
&\quad \times \left\{ (\not{p}_N - \not{p}_h + \not{k} + M) \left[ 1 - \frac{2k p_N}{D} + \frac{2k p_h}{D} \right] \right. \\
&\quad \left. + (\not{p}_N - \not{p}_{h'} + \not{k} + M) \left[ 1 - \frac{2k p_N}{D} + \frac{2k p_{h'}}{D} \right] \right\} \\
&\quad \times (\not{p}_N + \not{k} + M) \left[ 1 - \frac{2k p_N}{D} \right] P_R u(p_N) \\
&= \frac{g_N^2 g_X^2}{2} \bar{u}(p_{N'}) P_L \left\{ 2 [2B_4 - 24C_5 + 2M^2 A_4 - 12M^2 B_5] \not{p}_N \right. \\
&\quad \left. + [2B_4 + 12C_5 - M^2 A_4 + 6M^2 B_5] \not{p}_h \right.
\end{aligned}$$

$$\begin{aligned}
& + [2B_4 + 12C_5 - M^2 A_4 + 6M^2 B_5] \not{p}_{h'} \\
& + 2 [4B_4 - 12C_5 + M^2 A_4 - 6M^2 B_5] \not{p}_{N'} \Big\} u(p_N) \\
= & \frac{ig_N^2 g_X^2}{96\pi^2 M^2} \bar{u}(p_{N'}) P_L \left\{ \not{p}_N - \not{p}_h - \not{p}_{h'} - \not{p}_{N'} \right\} u(p_N) = 0, \tag{B.9}
\end{aligned}$$

by virtue of the momentum conservation. Thus, we get:

$$\begin{aligned}
i\mathcal{M}_{UV} = i\mathcal{M}_{UV}^c &= g_N^2 \lambda_{\varphi H} \bar{u}(p_{N'}) P_L \left\{ \int \frac{d^4 k}{(2\pi)^4} \frac{1}{D^3} (\not{p}_N + \not{k} + M) \right. \\
& \quad \left. \times \left[ 1 - \frac{2k p_N}{D} \right] \left[ 1 - \frac{2k(p_N - p_{N'})}{D} \right] \right\} P_R u(p_N) \\
&= g_N^2 \lambda_{\varphi H} \bar{u}(p_{N'}) P_L \left\{ [A_3 - 4B_4] \not{p}_N + 2B_4 \not{p}_{N'} \right\} u(p_N) \\
&= -\frac{ig_N^2 \lambda_{\varphi H}}{96\pi^2 M^2} \bar{u}(p_{N'}) P_L \left\{ \not{p}_N + \not{p}_{N'} \right\} u(p_N). \tag{B.10}
\end{aligned}$$

## B.6 Amplitude for two Higgses and one $W^3$

The relevant diagram in the UV is the diagram (a) in Fig. 4. We have:

$$\begin{aligned}
i\mathcal{M}_{UV} &= -\frac{gg_N^2 g_X^2}{2} \bar{u}(p_{N'}) P_L \int \frac{d^4 k}{(2\pi)^4} \frac{1}{D^5} (\not{k} + M)^2 \gamma^\mu (\not{k} + M)^2 P_R u(p_N) \epsilon_\mu^*(p_{W^3}) \\
&= -\frac{gg_N^2 g_X^2}{2} \bar{u}(p_{N'}) P_L (24C_5 + M^4 A_5) \gamma^\mu u(p_N) \epsilon_\mu^*(p_{W^3}) \\
&= \frac{igg_N^2 g_X^2}{96\pi^2 M^2} \bar{u}(p_{N'}) P_L \gamma^\mu u(p_N) \epsilon_\mu^*(p_{W^3}). \tag{B.11}
\end{aligned}$$

## B.7 Amplitude for three Higgses and no gauge bosons

This UV amplitude is represented by the diagrams (b) and (c) in Fig. 4. We have:

$$\begin{aligned}
i\mathcal{M}_{UV}^b &= -\frac{3g_N g_X^3 g_L}{\sqrt{2}} \bar{u}(p_N) P_L \int \frac{d^4 k}{(2\pi)^4} \frac{1}{D^5} (\not{k} + M)^4 P_L u(p_\nu) \\
&= -\frac{3g_N g_X^3 g_L}{\sqrt{2}} \bar{u}(p_N) P_L (24C_5 + 24M^2 B_5 + M^4 A_5) u(p_\nu) \\
&= -\frac{ig_N g_X^3 g_L}{32\sqrt{2}\pi^2 M^2} \bar{u}(p_N) P_L u(p_\nu), \tag{B.12}
\end{aligned}$$

$$\begin{aligned}
i\mathcal{M}_{UV}^c &= -\frac{3\lambda_{\varphi H}g_N g_X g_L}{\sqrt{2}} \bar{u}(p_N) P_L \int \frac{d^4k}{(2\pi)^4} \frac{1}{D^4} (\not{k} + M)^2 P_L u(p_\nu) \\
&= -\frac{3\lambda_{\varphi H}g_N g_X g_L}{\sqrt{2}} \bar{u}(p_N) P_L (4B_4 + M^2 A_4) u(p_\nu) \\
&= \frac{i\lambda_{\varphi H}g_N g_X g_L}{32\sqrt{2}\pi^2 M^2} \bar{u}(p_N) P_L u(p_\nu).
\end{aligned} \tag{B.13}$$

Finally,

$$i\mathcal{M}_{UV} = i\mathcal{M}_{UV}^b + i\mathcal{M}_{UV}^c = \frac{ig_N g_X g_L}{32\sqrt{2}\pi^2 M^2} (\lambda_{\varphi H} - g_X^2) \bar{u}(p_N) P_L u(p_\nu). \tag{B.14}$$

## B.8 Amplitude for four $N$ fermions

This UV amplitude is depicted by the diagram (a) in Fig. 5 (note that there is a second diagram with opposite sign due to the exchange of identical fermions). We have:

$$\begin{aligned}
i\mathcal{M}_{UV} &= g_N^4 \int \frac{d^4k}{(2\pi)^4} \frac{1}{D^4} \left\{ [\bar{u}(p_3) P_L (\not{k} + M) P_R u(p_1)] [\bar{u}(p_4) P_L (\not{k} + M) P_R u(p_2)] \right. \\
&\quad \left. - [\bar{u}(p_4) (\not{k} + M) u(p_1)] [\bar{u}(p_3) (\not{k} + M) P_R u(p_2)] \right\} \\
&= g_N^4 B_4 \left\{ [\bar{u}(p_3) \gamma^\mu P_R u(p_1)] [\bar{u}(p_4) \gamma_\mu P_R u(p_2)] \right. \\
&\quad \left. - [\bar{u}(p_4) \gamma^\mu P_R u(p_1)] [\bar{u}(p_3) \gamma_\mu P_R u(p_2)] \right\} \\
&= 2g_N^4 B_4 [\bar{u}(p_3) \gamma^\mu P_R u(p_1)] [\bar{u}(p_4) \gamma_\mu P_R u(p_2)] \\
&= -\frac{ig_N^4}{96\pi^2 M^2} [\bar{u}(p_3) \gamma^\mu P_R u(p_1)] [\bar{u}(p_4) \gamma_\mu P_R u(p_2)].
\end{aligned} \tag{B.15}$$

In the penultimate step, we have rearranged the spinors using a Fierz identity.

## B.9 Amplitude for two $N$ fermions and two neutrinos

This amplitude in the UV is given by the diagram (b) in Fig. 5. We have:

$$\begin{aligned}
i\mathcal{M}_{UV} &= g_N^2 g_L^2 \int \frac{d^4k}{(2\pi)^4} \frac{1}{D^4} [\bar{u}(p_{\nu'}) P_R (\not{k} + M) P_L u(p_\nu)] [\bar{u}(p_{N'}) P_L (\not{k} + M) P_R u(p_N)] \\
&= g_N^2 g_L^2 B_4 [\bar{u}(p_{\nu'}) \gamma^\mu P_L u(p_\nu)] [\bar{u}(p_{N'}) \gamma_\mu P_R u(p_N)] \\
&= -\frac{ig_N^2 g_L^2}{192\pi^2 M^2} [\bar{u}(p_{\nu'}) \gamma^\mu P_L u(p_\nu)] [\bar{u}(p_{N'}) \gamma_\mu P_R u(p_N)].
\end{aligned} \tag{B.16}$$

## B.10 Amplitude for six Higgses

The relevant UV diagrams are depicted in Fig. 6. We have:

$$\begin{aligned} i\mathcal{M}_{UV}^a &= -30g_X^6 \int \frac{d^4k}{(2\pi)^4} \frac{\text{Tr}[(\not{k} + M)^6]}{D^6} \\ &= -120g_X^6 [D_6 + 360M^2C_6 + 60M^4B_6 + M^6A_6] = -\frac{3ig_X^6}{4\pi^2M^2}, \end{aligned} \quad (\text{B.17})$$

(the minus sign comes from the loop of fermions; note also that there are 240 diagrams, which divided by  $\sqrt{2}^6$  gives 30<sup>6</sup>) as well as

$$i\mathcal{M}_{UV}^b = 30\lambda_{\varphi H}^3 \int \frac{d^4k}{(2\pi)^4} \frac{1}{D^3} = 30\lambda_{\varphi H}^3 A_3 = -\frac{15i\lambda_{\varphi H}^3}{16\pi^2M^2}, \quad (\text{B.18})$$

from where:

$$i\mathcal{M}_{UV} = i\mathcal{M}_{UV}^a + i\mathcal{M}_{UV}^b = -\frac{3i(4g_X^6 + 5\lambda_{\varphi H}^3)}{16\pi^2M^2}. \quad (\text{B.19})$$

## C Matching the $\nu$ SMEFT onto the $\nu$ LEFT and anomalous dimensions

The full list of dimension-six operators in the  $\nu$ LEFT involving  $N$  is shown in Tab. 3. (Those not involving  $N$  can be found in Ref. [15].) The following relations hold at the EW matching scale (note that we are ignoring family indices):

$$\frac{\alpha_{N\gamma}}{v} = \frac{v}{\sqrt{2}\Lambda^2} (\alpha_{NBCW} + \alpha_{NWSW}), \quad (\text{C.1}) \quad \frac{\alpha_{NN}^{V,RR}}{v^2} = \frac{\alpha_{NN}}{\Lambda^2}, \quad (\text{C.2})$$

$$\frac{\alpha_{eN}^{V,RR}}{v^2} = \frac{\alpha_{eN}}{\Lambda^2} - \frac{g_Z^2 Z_{eR} Z_N}{m_Z^2}, \quad (\text{C.3}) \quad \frac{\alpha_{uN}^{V,RR}}{v^2} = \frac{\alpha_{uN}}{\Lambda^2} - \frac{g_Z^2 Z_{uR} Z_N}{m_Z^2}, \quad (\text{C.4})$$

$$\frac{\alpha_{dN}^{V,RR}}{v^2} = \frac{\alpha_{dN}}{\Lambda^2} - \frac{g_Z^2 Z_{dR} Z_N}{m_Z^2}, \quad (\text{C.5}) \quad \frac{\alpha_{duNe}^{V,RR}}{v^2} = \frac{\alpha_{duNe}}{\Lambda^2}, \quad (\text{C.6})$$

$$\frac{\alpha_{\nu N}^{V,LR}}{v^2} = \frac{\alpha_{LN}}{\Lambda^2} - \frac{g_Z^2 Z_{\nu L} Z_N}{m_Z^2}, \quad (\text{C.7}) \quad \frac{\alpha_{eN}^{V,LR}}{v^2} = \frac{\alpha_{LN}}{\Lambda^2} - \frac{g_Z^2 Z_{eL} Z_N}{m_Z^2}, \quad (\text{C.8})$$

$$\frac{\alpha_{uN}^{V,LR}}{v^2} = \frac{\alpha_{QN}}{\Lambda^2} - \frac{g_Z^2 Z_{uL} Z_N}{m_Z^2}, \quad (\text{C.9}) \quad \frac{\alpha_{dN}^{V,LR}}{v^2} = \frac{\alpha_{QN}}{\Lambda^2} - \frac{g_Z^2 Z_{dL} Z_N}{m_Z^2}, \quad (\text{C.10})$$

---

<sup>6</sup>Here we have also used the fact that

$$D_n \equiv \int \frac{d^d k}{(4\pi)^d} \frac{k^6}{(k^2 - M^2)^n} = -\frac{i(-1)^n d(d+2)(d+4)}{8(4\pi)^{d/2}} \frac{\Gamma(n - \frac{d}{2} - 3)}{\Gamma(n)} \frac{1}{M^{2n-d-6}}.$$

Dipole	$\mathcal{O}_{N\gamma} = \bar{\nu}_L \sigma^{\mu\nu} N A_{\mu\nu}$	
RRRR	$\mathcal{O}_{NN}^{V,RR} = (\bar{N} \gamma_\mu N)(\bar{N} \gamma^\mu N)$	
	$\mathcal{O}_{eN}^{V,RR} = (\bar{e}_R \gamma_\mu e_R)(\bar{N} \gamma^\mu N)$	$\mathcal{O}_{uN}^{V,RR} = (\bar{u}_R \gamma_\mu u_R)(\bar{N} \gamma^\mu N)$
	$\mathcal{O}_{dN}^{V,RR} = (\bar{d}_R \gamma_\mu d_R)(\bar{N} \gamma^\mu N)$	$\mathcal{O}_{duNe}^{V,RR} = (\bar{d}_R \gamma_\mu u_R)(\bar{N} \gamma^\mu e_R)$
LLRR	$\mathcal{O}_{\nu N}^{V,LR} = (\bar{\nu}_L \gamma_\mu \nu_L)(\bar{N} \gamma^\mu N)$	$\mathcal{O}_{eN}^{V,LR} = (\bar{e}_L \gamma_\mu e_L)(\bar{N} \gamma^\mu N)$
	$\mathcal{O}_{uN}^{V,LR} = (\bar{u}_L \gamma_\mu u_L)(\bar{N} \gamma^\mu N)$	$\mathcal{O}_{dN}^{V,LR} = (\bar{d}_L \gamma_\mu d_L)(\bar{N} \gamma^\mu N)$
	$\mathcal{O}_{duNe}^{V,LR} = (\bar{d}_L \gamma_\mu u_L)(\bar{N} \gamma^\mu e_R)$	
LRRR	$\mathcal{O}_{NN}^{S,RR} = (\bar{\nu}_L N)(\bar{\nu}_L N)$	
	$\mathcal{O}_{eN}^{S,RR} = (\bar{e}_L e_R)(\bar{\nu}_L N)$	$\mathcal{O}_{eN}^{T,RR} = (\bar{e}_L \sigma^{\mu\nu} e_R)(\bar{\nu}_L \sigma_{\mu\nu} N)$
	$\mathcal{O}_{uN}^{S,RR} = (\bar{u}_L u_R)(\bar{\nu}_L N)$	$\mathcal{O}_{uN}^{T,RR} = (\bar{u}_L \sigma^{\mu\nu} u_R)(\bar{\nu}_L \sigma_{\mu\nu} N)$
	$\mathcal{O}_{dN}^{S,RR} = (\bar{d}_L d_R)(\bar{\nu}_L N)$	$\mathcal{O}_{dN}^{T,RR} = (\bar{d}_L \sigma^{\mu\nu} d_R)(\bar{\nu}_L \sigma_{\mu\nu} N)$
	$\mathcal{O}_{duNe}^{S,RR} = (\bar{e}_L N)(\bar{u}_L d_R)$	$\mathcal{O}_{duNe}^{T,RR} = (\bar{e}_L \sigma^{\mu\nu} N)(\bar{u}_L \sigma_{\mu\nu} d_R)$
	$\mathcal{O}_{eN}^{S,RL} = (\bar{e}_L e_R)(\bar{N} \nu_L)$	$\mathcal{O}_{uN}^{S,RL} = (\bar{u}_L u_R)(\bar{N} \nu_L)$
	$\mathcal{O}_{dN}^{S,RL} = (\bar{d}_L d_R)(\bar{N} \nu_L)$	$\mathcal{O}_{duNe}^{S,RL} = (\bar{e}_L N)(\bar{u}_R d_L)$

Table 3: List of  $\nu$ LEFT operators involving  $N$ . The addition of h.c. is implied when needed. The notation follows that of Ref. [15], although we have not tried to minimise the number of operators involving  $\sigma_{\mu\nu}$ .

$$\frac{\alpha_{duNe}^{V,LR}}{v^2} = -\frac{g^2 W_N}{2m_W^2}, \quad (\text{C.11}) \quad \alpha_{NN}^{S,RR} = 0, \quad (\text{C.12})$$

$$\frac{\alpha_{eN}^{S,RR}}{v^2} = \frac{3\alpha_{LNLe}}{2\Lambda^2}, \quad (\text{C.13}) \quad \frac{\alpha_{eN}^{T,RR}}{v^2} = \frac{\alpha_{LNLe}}{8\Lambda^2}, \quad (\text{C.14})$$

$$\alpha_{uN}^{S,RR} = 0, \quad (\text{C.15}) \quad \alpha_{uN}^{T,RR} = 0, \quad (\text{C.16})$$

$$\frac{\alpha_{dN}^{S,RR}}{v^2} = \frac{\alpha_{LNQd}}{\Lambda^2} - \frac{\alpha_{LdQN}}{2\Lambda^2}, \quad (\text{C.17}) \quad \frac{\alpha_{dN}^{T,RR}}{v^2} = -\frac{\alpha_{LdQN}}{8\Lambda^2}, \quad (\text{C.18})$$

$$\frac{\alpha_{duNe}^{S,RR}}{v^2} = \frac{\alpha_{LdQN}}{2\Lambda^2} - \frac{\alpha_{LNQd}}{\Lambda^2}, \quad (\text{C.19}) \quad \frac{\alpha_{duNe}^{T,RR}}{v^2} = \frac{\alpha_{LdQN}}{8\Lambda^2}, \quad (\text{C.20})$$

$$\frac{\alpha_{eN}^{S,RL}}{v^2} = \frac{g^2 W_N}{m_W^2}, \quad (\text{C.21}) \quad \frac{\alpha_{uN}^{S,RL}}{v^2} = \frac{\alpha_{QuNL}}{\Lambda^2}, \quad (\text{C.22})$$

$$\alpha_{dN}^{S,RL} = 0, \quad (\text{C.23}) \quad \frac{\alpha_{duNe}^{S,RL}}{v^2} = \frac{\alpha_{QuNL}}{\Lambda^2}. \quad (\text{C.24})$$



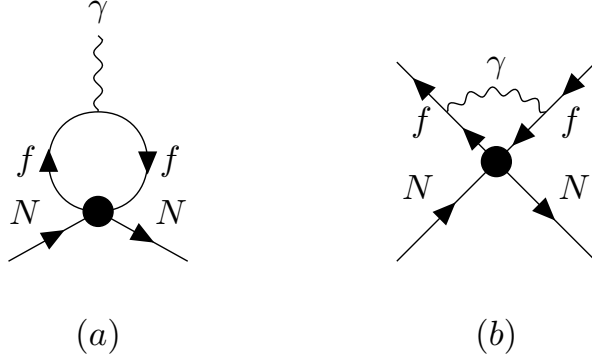


Figure 8: (a) Renormalisation of the operator  $\partial^\nu A_{\mu\nu} \bar{N} \gamma^\mu N$  by four-fermions. It generates other four-fermions upon using the equations of motion. (b) Self-renormalisation of four-fermions.

The coupling  $g_Z$  is defined as  $g_Z = e/(s_W c_W)$ . We have also defined  $Z_{\psi_{SM}} = T_3 - Q s_W^2$  and  $Z_N = -\alpha_{HN} v^2 / (2\Lambda^2)$  as well as  $W_N = \alpha_{HN} e v^2 / (2\Lambda^2)$ . Note that we can neglect EFT effects in the non  $N$  fermion couplings to the  $Z$  and  $W$  because they would lead to dimension-eight contributions.

In our case, the only operators that are generated are the dipole as well as LL and RR four-fermions with two  $N$ s. They renormalise due to quantum corrections depicted by the diagrams in Fig. 8. Using the notation

$$\dot{\alpha} \equiv 16\pi^2 \mu \frac{d\alpha}{d\mu}, \quad (\text{C.25})$$

we obtain:

$$\dot{\alpha}_{N\gamma} = \frac{4}{3} (3q_e^2 + 3N_c q_d^2 + 2N_c q_u^2) e^2 \alpha_{N\gamma}, \quad (\text{C.26})$$

$$\begin{aligned} \dot{\alpha}_{\psi N}^{V,RR} = \frac{4}{3} e^2 q_\psi \left[ N_c q_u \left( \alpha_{uN}^{V,RR} + \alpha_{uN}^{V,LR} \right) + N_c q_d \left( \alpha_{dN}^{V,RR} + \alpha_{dN}^{V,LR} \right) \right. \\ \left. + q_e \left( \alpha_{eN}^{V,RR} + \alpha_{eN}^{V,LR} \right) \right], \end{aligned} \quad (\text{C.27})$$

$$\begin{aligned} \dot{\alpha}_{\psi N}^{V,LR} = \frac{4}{3} e^2 q_\psi \left[ N_c q_u \left( \alpha_{uN}^{V,RR} + \alpha_{uN}^{V,LR} \right) + N_c q_d \left( \alpha_{dN}^{V,RR} + \alpha_{dN}^{V,LR} \right) \right. \\ \left. + q_e \left( \alpha_{eN}^{V,RR} + \alpha_{eN}^{V,LR} \right) \right], \end{aligned} \quad (\text{C.28})$$

for  $\psi = \nu, N, e, u, d$ . The non-vanishing electric charges are  $q_e = -1$ ,  $q_u = 2/3$  and  $q_d = -1/3$ . This automatically implies that  $\dot{\alpha}_{NN}^{V,RR} = 0$  and  $\dot{\alpha}_{\nu N}^{V,LR} = 0$ ; *i.e.* these operators do not renormalise.

## References

- [1] W. Buchmuller and D. Wyler, *Effective Lagrangian Analysis of New Interactions and Flavor Conservation*, *Nucl. Phys.* **B268** (1986) 621.
- [2] B. Grzadkowski, M. Iskrzynski, M. Misiak and J. Rosiek, *Dimension-Six Terms in the Standard Model Lagrangian*, *JHEP* **10** (2010) 085 [1008.4884].
- [3] I. Brivio and M. Trott, *The Standard Model as an Effective Field Theory*, *Phys. Rept.* **793** (2019) 1 [1706.08945].
- [4] F. del Aguila, S. Bar-Shalom, A. Soni and J. Wudka, *Heavy Majorana Neutrinos in the Effective Lagrangian Description: Application to Hadron Colliders*, *Phys. Lett.* **B670** (2009) 399 [0806.0876].
- [5] Y. Liao and X.-D. Ma, *Operators up to Dimension Seven in Standard Model Effective Field Theory Extended with Sterile Neutrinos*, *Phys. Rev.* **D96** (2017) 015012 [1612.04527].
- [6] R. Franceschini, G. F. Giudice, J. F. Kamenik, M. McCullough, F. Riva, A. Strumia et al., *Digamma, what next?*, *JHEP* **07** (2016) 150 [1604.06446].
- [7] B. Gripaios and D. Sutherland, *An operator basis for the Standard Model with an added scalar singlet*, *JHEP* **08** (2016) 103 [1604.07365].
- [8] Anisha, S. Das Bakshi, J. Chakraborty and S. Prakash, *Hilbert Series and Plethystics: Paving the path towards 2HDM- and MLRSM-EFT*, *JHEP* **09** (2019) 035 [1905.11047].
- [9] G. Durieux, F. Maltoni and C. Zhang, *Global approach to top-quark flavor-changing interactions*, *Phys. Rev.* **D91** (2015) 074017 [1412.7166].
- [10] M. Chala, J. Santiago and M. Spannowsky, *Constraining four-fermion operators using rare top decays*, *JHEP* **04** (2019) 014 [1809.09624].
- [11] S. Banerjee, M. Chala and M. Spannowsky, *Top quark FCNCs in extended Higgs sectors*, *Eur. Phys. J.* **C78** (2018) 683 [1806.02836].
- [12] J. Alcaide, S. Banerjee, M. Chala and A. Titov, *Probes of the Standard Model effective field theory extended with a right-handed neutrino*, *JHEP* **08** (2019) 031 [1905.11375].
- [13] A. Caputo, P. Hernandez, J. Lopez-Pavon and J. Salvado, *The seesaw portal in testable models of neutrino masses*, *JHEP* **06** (2017) 112 [1704.08721].

- [14] J. M. Butterworth, M. Chala, C. Englert, M. Spannowsky and A. Titov, *Higgs phenomenology as a probe of sterile neutrinos*, *Phys. Rev.* **D100** (2019) 115019 [1909.04665].
- [15] E. E. Jenkins, A. V. Manohar and P. Stoffer, *Low-Energy Effective Field Theory below the Electroweak Scale: Operators and Matching*, *JHEP* **03** (2018) 016 [1709.04486].
- [16] W. Dekens and P. Stoffer, *Low-energy effective field theory below the electroweak scale: matching at one loop*, *JHEP* **10** (2019) 197 [1908.05295].
- [17] E. E. Jenkins, A. V. Manohar and M. Trott, *Renormalization Group Evolution of the Standard Model Dimension Six Operators I: Formalism and lambda Dependence*, *JHEP* **10** (2013) 087 [1308.2627].
- [18] E. E. Jenkins, A. V. Manohar and M. Trott, *Renormalization Group Evolution of the Standard Model Dimension Six Operators II: Yukawa Dependence*, *JHEP* **01** (2014) 035 [1310.4838].
- [19] R. Alonso, E. E. Jenkins, A. V. Manohar and M. Trott, *Renormalization Group Evolution of the Standard Model Dimension Six Operators III: Gauge Coupling Dependence and Phenomenology*, *JHEP* **04** (2014) 159 [1312.2014].
- [20] E. E. Jenkins, A. V. Manohar and P. Stoffer, *Low-Energy Effective Field Theory below the Electroweak Scale: Anomalous Dimensions*, *JHEP* **01** (2018) 084 [1711.05270].
- [21] A. Aparici, K. Kim, A. Santamaria and J. Wudka, *Right-handed neutrino magnetic moments*, *Phys. Rev.* **D80** (2009) 013010 [0904.3244].
- [22] S. Bhattacharya and J. Wudka, *Dimension-seven operators in the standard model with right handed neutrinos*, *Phys. Rev.* **D94** (2016) 055022 [1505.05264].
- [23] B. Henning, X. Lu and H. Murayama, *How to use the Standard Model effective field theory*, *JHEP* **01** (2016) 023 [1412.1837].
- [24] B. Henning, X. Lu and H. Murayama, *One-loop Matching and Running with Covariant Derivative Expansion*, *JHEP* **01** (2018) 123 [1604.01019].
- [25] S. A. R. Ellis, J. Quevillon, T. You and Z. Zhang, *Mixed heavy–light matching in the Universal One-Loop Effective Action*, *Phys. Lett.* **B762** (2016) 166 [1604.02445].
- [26] J. Fuentes-Martin, J. Portoles and P. Ruiz-Femenia, *Integrating out heavy particles with functional methods: a simplified framework*, *JHEP* **09** (2016) 156 [1607.02142].

- [27] Z. Zhang, *Covariant diagrams for one-loop matching*, *JHEP* **05** (2017) 152 [1610.00710].
- [28] S. A. R. Ellis, J. Quevillon, T. You and Z. Zhang, *Extending the Universal One-Loop Effective Action: Heavy-Light Coefficients*, *JHEP* **08** (2017) 054 [1706.07765].
- [29] F. del Aguila, Z. Kunszt and J. Santiago, *One-loop effective lagrangians after matching*, *Eur. Phys. J.* **C76** (2016) 244 [1602.00126].
- [30] J. C. Criado, *MatchingTools: a Python library for symbolic effective field theory calculations*, *Comput. Phys. Commun.* **227** (2018) 42 [1710.06445].
- [31] I. Brivio et al., *Computing Tools for the SMEFT*, in *Computing Tools for the SMEFT*, J. Aebischer, M. Fael, A. Lenz, M. Spannowsky and J. Virto, eds., 2019, 1910.11003.
- [32] M. Boggia, R. Gomez-Ambrosio and G. Passarino, *Low energy behaviour of standard model extensions*, *JHEP* **05** (2016) 162 [1603.03660].
- [33] M. Jiang, N. Craig, Y.-Y. Li and D. Sutherland, *Complete One-Loop Matching for a Singlet Scalar in the Standard Model EFT*, *JHEP* **02** (2019) 031 [1811.08878].
- [34] M. S. Bilenky and A. Santamaria, *One loop effective Lagrangian for a standard model with a heavy charged scalar singlet*, *Nucl. Phys.* **B420** (1994) 47 [hep-ph/9310302].
- [35] J. C. Criado, *BasisGen: automatic generation of operator bases*, *Eur. Phys. J.* **C79** (2019) 256 [1901.03501].
- [36] R. M. Fonseca, *Enumerating the operators of an effective field theory*, 1907.12584.
- [37] J. Ellis, *TikZ-Feynman: Feynman diagrams with TikZ*, *Comput. Phys. Commun.* **210** (2017) 103 [1601.05437].
- [38] PARTICLE DATA GROUP collaboration, *Review of Particle Physics*, *Phys. Rev.* **D98** (2018) 030001.
- [39] L. Duarte, J. Peressutti and O. A. Sampayo, *Majorana neutrino decay in an Effective Approach*, *Phys. Rev.* **D92** (2015) 093002 [1508.01588].
- [40] L3 collaboration, *Search for new physics in energetic single photon production in  $e^+e^-$  annihilation at the Z resonance*, *Phys. Lett.* **B412** (1997) 201.

- [41] CMS collaboration, *Search for new physics in final states with a single photon and missing transverse momentum in proton-proton collisions at  $\sqrt{s} = 13$  TeV*, *JHEP* **02** (2019) 074 [1810.00196].
- [42] J. M. Butterworth, D. Grellscheid, M. Krämer, B. Sarrazin and D. Yallup, *Constraining new physics with collider measurements of Standard Model signatures*, *JHEP* **03** (2017) 078 [1606.05296].
- [43] M. Chala, C. Krause and G. Nardini, *Signals of the electroweak phase transition at colliders and gravitational wave observatories*, *JHEP* **07** (2018) 062 [1802.02168].
- [44] L. Duarte, J. Peressutti and O. A. Sampayo, *Not-that-heavy Majorana neutrino signals at the LHC*, *J. Phys.* **G45** (2018) 025001 [1610.03894].
- [45] B. C. Canas, O. G. Miranda, A. Parada, M. Tortola and J. W. F. Valle, *Updating neutrino magnetic moment constraints*, *Phys. Lett.* **B753** (2016) 191 [1510.01684].
- [46] M. Redi, *Leptons in Composite MFV*, *JHEP* **09** (2013) 060 [1306.1525].
- [47] Q.-H. Cao, G. Li, K.-P. Xie and J. Zhang, *Searching for Weak Singlet Charged Scalar at the Large Hadron Collider*, *Phys. Rev.* **D97** (2018) 115036 [1711.02113].
- [48] ATLAS collaboration, *Search for electroweak production of supersymmetric particles in final states with two or three leptons at  $\sqrt{s} = 13$  TeV with the ATLAS detector*, *Eur. Phys. J.* **C78** (2018) 995 [1803.02762].
- [49] J. Alcaide and N. I. Mileo, *LHC sensitivity to singly-charged scalars decaying into electrons and muons*, 1906.08685.